Photometric and polarimetric studies of three W UMa-type binaries: FZ Ori, V407 Peg and LP UMa

Vinod Prasad, J. C. Pandey, M. K. Patel & D. C. Srivastava

Astrophysics and Space Science
An International Journal of Astronomy, Astrophysics and Space Science

ISSN 0004-640X
Volume 353
Number 2

Astrophys Space Sci (2014) 353:575-594
DOI 10.1007/s10509-014-2088-3

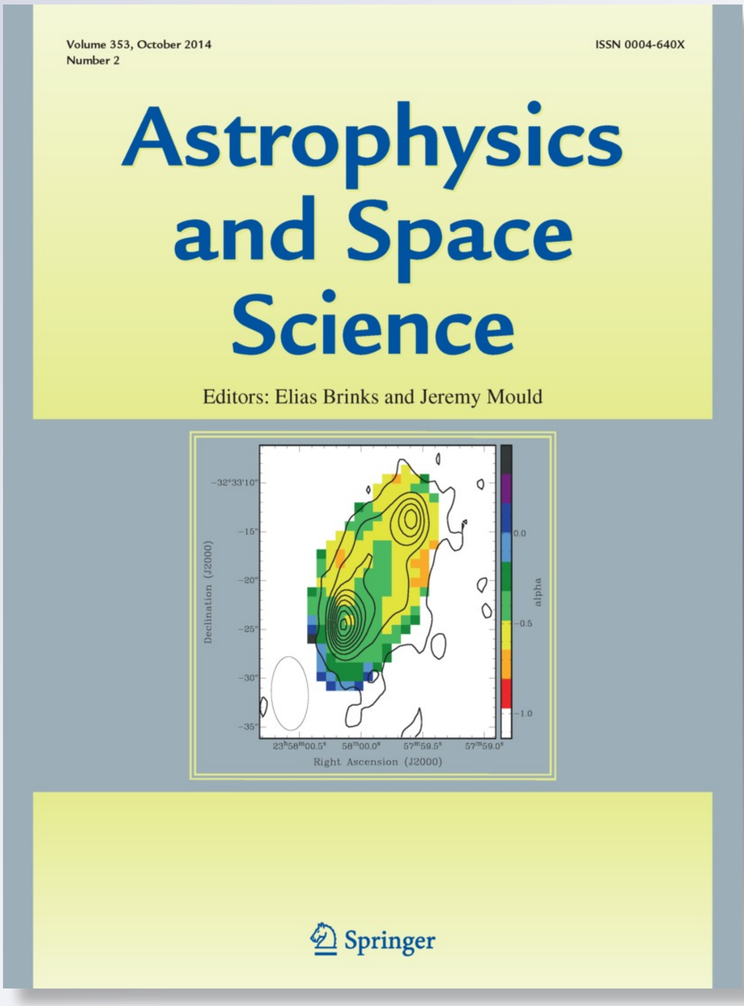

Springer

Astrophys Space Sci (2014) 353:575–594
DOI 10.1007/s10509-014-2088-3

ORIGINAL ARTICLE

Photometric and polarimetric studies of three W UMa-type binaries: FZ Ori, V407 Peg and LP UMa

Vinod Prasad · J.C. Pandey · M.K. Patel · D.C. Srivastava

Received: 6 March 2014 / Accepted: 28 July 2014 / Published online: 12 August 2014

Abstract We present analyses of new optical photometric observations of three W UMa-type contact binaries FZ Ori, V407 Peg and LP UMa. Results from the first polarimetric observations of the FZ Ori and V407 Peg are also presented. The periods of FZ Ori, V407 Peg and LP UMa are derived to be 0.399986, 0.636884 and 0.309898 d, respectively. The $O-C$ analyses indicate that the orbital periods of FZ Ori and LP UMa have increased with the rate of 2.28×10^{-8} and 1.25×10^{-6} d yr^{-1}, respectively and which is explained by transfer of mass between the components. In addition to the secularly increasing rate of orbital period, it was found that the period of FZ Ori has varied in sinusoidal way with oscillation period of ∼30.1 yr. The period of oscillations are most likely to be explained by the light-time effect due to the presence of a tertiary companion. Small asymmetries have been seen around the primary and secondary maxima of light curves of all three systems, which is probably due to the presence of cool/hot spots on the components. The light curves of all three systems are analysed by using Wilson-Devinney code (WD) and the fundamental parameters of these systems have been derived. The present analyses show that FZ Ori is a W-subtype, and V407 Peg and LP UMa are A-subtype of the W UMa-type contact binary systems. The polarimetric observations in B, V, R and I bands, yield average values of polarization to be 0.26 ± 0.03, 0.22 ± 0.02, 0.22 ± 0.03 and 0.22 ± 0.05 per cent for FZ Ori and 0.21 ± 0.02, 0.29 ± 0.03, 0.31 ± 0.01 and 0.31 ± 0.04 per cent for V407 Peg, respectively.

Keywords Binaries · Close-binaries · Eclipsing-stars · Evolution-stars · Individual (FZ Ori, V407 Peg and LP UMa)

V. Prasad (✉) · M.K. Patel · D.C. Srivastava
Department of Physics, DDU Gorakhpur University, Gorakhpur 273009, India
e-mail: vinod.pdr83@gmail.com

M.K. Patel
e-mail: patelmanoj79@gmail.com

D.C. Srivastava
e-mail: dcs.gkp@gmail.com

J.C. Pandey
Aryabhatta Research Institute of Observational Sciences, Nainital 263002, India
e-mail: jeewan@aries.res.in

1 Introduction

W Ursae Majoris (W UMa)-type variable stars are overcontact eclipsing binary stars whose light curves have strongly curved maxima and minima that are nearly equal in depth. Binnendijk (1970) divided EW stars into two sub-classes which he called A-type and W-type. In the A-type systems the larger component has the higher temperature whereas in the W-type systems the smaller component has the higher temperature. Observationally it has been found that the A-type systems tend to have low mass ratios ($q < 0.3$) and spectral type from A to F. W-type systems usually have mass ratios $q > 0.3$ and spectral types of G or K. Most light curves of W Ursae Majoris binaries usually show differences in the brightness of their maxima. This asymmetry is called the O'Connell effect (O'Connell 1951; Milone 1968) and has been of particular interest in understanding the light variations of W UMa binaries. It has also been reported that the shape of the light curves and the depth of eclipses vary with time for some systems. Thus, the asymmetric light curves of W UMa type systems may indicate the presence of starspots on one or both stars in the system. Many W UMa-type contact binaries show secular changes in orbital period which point to the possibility of gas streams and mass transfer between components. These instabilities are important when studying the evolution of close binaries. The changes in orbital period can be investigated by analyzing the residuals between observed and computed times of primary and secondary eclipses (the so-called $O-C$ plots). However, such analysis requires long term photometry. The effect of a stream on the total light intensity is usually small and sometimes difficult to find from photometric observations. The light scattered in the gaseous matter may be highly polarized (Piirola 1977). Therefore, polarimetric observations are important to derive the effect of gas stream and mass transfer rate (Shakhovskoi 1965; Oshchepkov 1978; Shakhovskoy and Antonyuk 2004).

The eclipsing binary FZ Orionis (= HD 288166) has been discovered to be a variable by Hoffmeister (1934). Figer (1983) and Le Brogne et al. (1984) suggested the system to be a W UMa type binary and reported a period of 0.3999860 d. The studies by Rukmini et al. (2001) and Byboth et al. (2004) indicate a slightly asymmetric light curve, which was explained in the latter paper by the presence of a spot on the primary component. The period variation of FZ Ori was analysed by El-Bassuny Alawy (1993). He reported a continuous period decrease at a rate of $dP/dt = 2.61 \times 10^{-5}$ day yr^{-1}, which is rather large for a contact binary. However, Qian and Ma (2001) have compiled many times of light minimum and they find out a period decrease rate of $dP/dt = 5.20 \times 10^{-7}$ day yr^{-1}, which is a typical value for W UMa type contact binaries. Recently, a period analysis was performed by Zasche et al. (2009) and they have found a steady period increase besides the cyclic variation of its orbital period. The results of the above three analyses for FZ Ori are in conflict with each other and the detailed analysis of this system is still lacking. The V407 Peg (= BD+14°5016) contact binary system was found to be variable during the Semi-Automatic Variability Search program at the Piwnice Observatory close to Torun, Poland (Maciejewski et al. 2002). Maciejewski et al. (2003) and Rucinski et al. (2008) had performed the spectroscopic analysis and obtained the preliminary solutions containing the mass ratio $q_{spec} = 0.256 \pm 0.006$. Deb and Singh (2011) have analyzed the publicly available V band observations of All Sky Automated Survey (ASAS) data (Pojmanski 1997, 2002) using the previous spectroscopically determined parameters as inputs and have found the photometric solution. Zasche (2011) has plotted $O-C$ diagram compiling all the published times of light minimum and found that the difference between primary and secondary minima is although visible but not significant. Recently, Lee et al. (2014) have determined the binary parameters of V407 Peg using their *BVR* bands observations. To obtain a unique set of the binary parameters, they have modeled the light curves simultaneously with the *RV* curves of Rucinski et al. (2008). The contact binary LP UMa (= GSC 3822-1056) was found to be variable by Martin (2000) and Biro (2000) during their observations of DW UMa (nova-like variable). Martin (2000) found LP UMa to be a δ Scuti variable. The colour indices of LP UMa indicate a mid G spectral type but this is inconsistent for a δ Scuti type variability. Biro (2000) has found, due to the evidence of light curve having alternate minima with different depths of the repeating cycles, LP UMa to be a β Lyr-type eclipsing binary system. Csizmadia et al. (2003), who performed the photometric analysis of LP UMa, obtained the preliminary solutions of the LP UMa containing the mass ratio, $q = 0.886 \pm 0.015$.

There is still lack of light curves of FZ Ori, V407 Peg and LP UMa in all optical bands in their analyses, therefore we decided to observe these systems for investigating the orbital and physical parameters. Further, no polarimetric observations are made till the date, which are useful to derive gas stream properties. In this paper, we report the multiband light curves analysis using our new photometric observations. We describe the observations and data reduction procedures in Sect. 2. In Sect. 3, we present the determination of ephemeris and period analysis. Sections 4 and 5 cover light curves and estimation of basic parameters. In Sect. 6, we present the analysis of the observations using Wilson-Devinney light curve modeling technique (WD code). The results of polarimetric observations are presented in Sect. 7. The results from this work are discussed and summarized in Sect. 8.

2 Observations and data reduction

2.1 Optical photometry

The photometric observations have been carried out in the U, B, V, R and I photometric filters during 2009 to 2011 at Aryabhatta Research Institute of observational sciencES (ARIES), Nainital, India, with a $2k \times 2k$ Wright CCD camera mounted on Cassegrain focus of the 104-cm Sampurnanand telescope. FZ Ori was observed for 16 nights, V407 Peg was observed for 14 nights and LP UMa was observed for 5 nights. The exposure times are ranging from 10 to 300 seconds depending upon individual system and observing conditions. The CCD system consists of $24 \times 24\mu^2$ size pixel. The gain and readout noise of CCD are $10e^-$/ADU and $5.3e^-$, respectively. To improve the signal-to-noise ratio, the observations have been taken in a binning mode of 2×2 pixel^2, where each super pixel corresponds to 0.72×0.72 arcsec^2. Several bias and twilight flat frames were also taken during each observing run. Bias subtraction, flat fielding and aperture photometry were performed using IRAF.[1]

[1]IRAF is distributed by National Optical Astronomy Observatories, USA; http://iraf.net.

Table 1 Basic information of comparison and check stars with the target stars: GSC 00119-00214 and GSC 00119-00771 for FZ Ori, and 2mass 23364621+1550367 and 2mass 23363947+1546301 for V407 Peg, and GSC 03822-00070 and 2mass 10342247+5852446 for LP UMa

Star	RA (J2000)	Dec (J2000)	B (mag)	V (mag)	J (mag)	H (mag)	K (mag)
FZ Ori	05 41 21.01	+02 36 22.98	11.18	10.53	9.639	9.366	9.297
GSC 00119-00214	05 41 17.59	+02 35 29.70	13.30	...	11.593	11.270	11.163
GSC 00119-00771	05 41 5.14	+02 37 11.90	15.50	...	12.630	12.204	12.062
V407 Peg	23 36 55.37	+15 48 6.43	9.79	9.45	8.498	8.376	8.317
2mass 23364621+1550367	23 36 46.21	+15 50 36.73	...	...	10.868	10.646	10.613
2mass 23363947+1546301	23 36 39.47	+15 46 30.14	...	...	12.132	11.759	11.704
LP UMa	10 33 57.78	+58 52 15.6	13.50	12.53	11.392	11.073	10.992
GSC 03822-00070	10 33 48.87	+58 52 31.0	13.92	13.29	11.797	11.358	11.308
2mass 10342247+5852446	10 34 22.47	+58 52 44.68	...	...	12.870	12.479	12.510

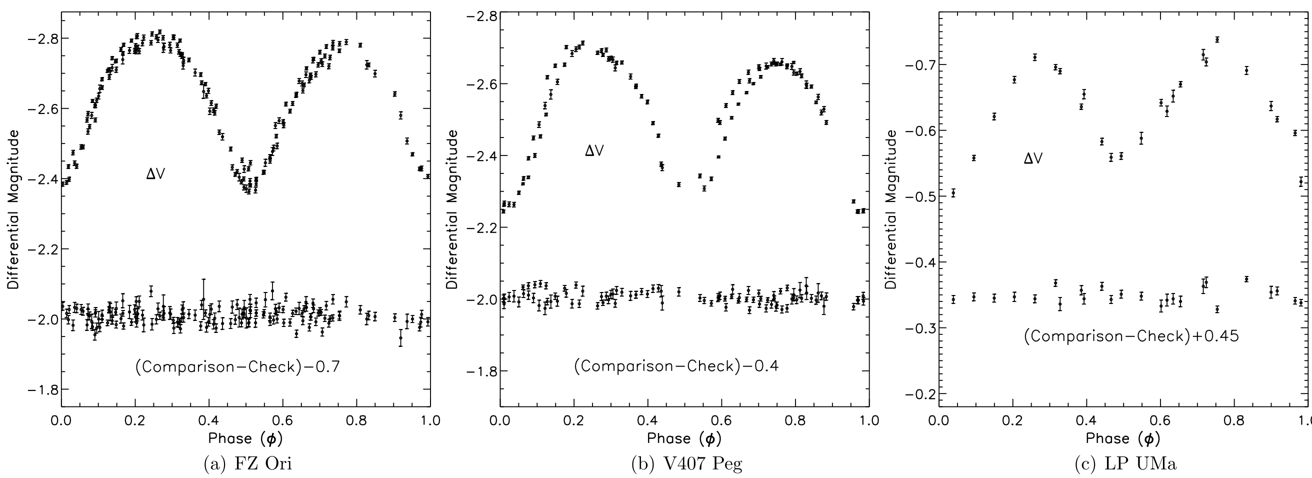

Fig. 1 Folded V-band light curves along with the comparison-check folded light curve in V band of (**a**) FZ Ori, (**b**) V407 Peg and (**c**) LP UMa

The comparison and check stars have been chosen respectively, as GSC 00119-00214, GSC 00119-00771 for FZ Ori, and 2mass 23364621+1550367, 2mass 23363947+1546301 for V407 Peg. GSC 03822-00070 and 2mass 10342247+5852446 are used as comparison and check stars for LP UMa. The basic parameters of the target, comparison and the check stars are given in Table 1. Differential photometry has been done in the sense of variable minus comparison star because all the program, comparison and check stars were in the same CCD frame. The comparison-check light curves in V band along with the V-band light curves of FZ Ori, V407 Peg and LP UMa are shown in Figs. 1(a), 1(b) and 1(c), respectively. The ephemeris used are given in Eqs. (2), (9) and (10), respectively. From the light curve, it is clear that the comparison and check stars were constant through out the observations. The nightly mean of standard deviation (σ) of different measures of comparison minus check stars in B, V, R and I bands were 0.023, 0.015, 0.017 and 0.016 for FZ Ori, 0.017, 0.014, 0.014 and 0.013 for V407 Peg, and 0.014, 0.008, 0.012 and 0.012 for LP UMa, respectively. Additionally, the σ of comparison—check stars in U band was 0.025 for V407 Peg.

2.2 Optical polarimetry

The broad-band B, V, R and I polarimetric observations of FZ Ori and V407 Peg were taken from ARIES Imaging Polarimeter (AIMPOL; Rautela et al. 2004) mounted on the cassegrain focus of the 104-cm Sampurnanand telescope of ARIES, Nainital, India. The star V407 Peg was observed on October 15, 16, 2010, November 26, 2010, and December 17, 2010, while, FZ Ori was observed on December 17, 18, 2010. The imaging has been done by using TK 1024×1024 pixel^2 CCD camera. Each pixel of the CCD corresponds to 1.73 arcsec and the field of view of the CCD is $\sim$8 arcmin in diameter. The gain and read out noise of the CCD are $11.98e^-$/ADU and $7.0e^-$, respectively. Detail about AIMPOL and its data reduction are given in Rautela et al. (2004), Medhi et al. (2007).

The AIMPOL consists of a half-wave plate (HWP) modulator and a Wollaston prism beam-splitter to produce ordinary and extraordinary images of each source. The images in the CCD frame are separated by 27 pixels along the north-south direction on the sky plane. The HWP is rotated at 22.5° intervals between exposures for linear polarimetry. Therefore, a single polarization measurement has been obtained from every four exposures (i.e. at the HWP position of

Table 2 Observed polarized and unpolarized standard stars

Filter	Polarized standard				Unpolarized standard	
	Schmidt et al. (1992)		Present work		Present work	
	P (%)	θ (°)	P (%)	θ (°)	q (%)	u (%)
HD 204827						
B	5.65 ± 0.02	58.20 ± 0.11	5.62 ± 0.01	58 ± 1		
V	5.32 ± 0.01	58.73 ± 0.08	5.49 ± 0.03	59 ± 1		
R	4.89 ± 0.03	59.10 ± 0.17	4.97 ± 0.06	59 ± 1		
I	4.19 ± 0.03	59.94 ± 0.20	4.10 ± 0.05	60 ± 1		
HD 25443					β UMa	
B	5.23 ± 0.09	134.28 ± 0.51	6.01 ± 0.60	133 ± 4	0.061	0.106
V	5.13 ± 0.06	134.23 ± 0.34	5.05 ± 0.09	134 ± 2	0.066	−0.009
R	4.73 ± 0.05	133.65 ± 0.28	4.82 ± 0.05	133 ± 1	−0.056	0.067
I	4.25 ± 0.04	134.21 ± 0.28	3.96 ± 0.14	135 ± 2	−0.003	−0.046
HD 19820					θ UMa	
B	4.70 ± 0.04	115.70 ± 0.22	4.48 ± 0.79	116 ± 6	−0.060	−0.113
V	4.79 ± 0.03	114.93 ± 0.17	4.70 ± 0.12	116 ± 2	−0.050	0.066
R	4.53 ± 0.03	114.46 ± 0.16	4.52 ± 0.06	115 ± 1	0.165	0.072
I	4.08 ± 0.02	114.48 ± 0.17	4.06 ± 0.03	115 ± 1	−0.193	−0.017

$0°$, $22°.5$, $45°$ and $67°.5$). Fluxes of ordinary (I_o) and extraordinary (I_e) beams for all the observed sources were extracted by standard aperture photometry after bias subtraction using the IRAF package. We have used the following relation to obtain the degree of polarization (P), defined as the fraction of the total linearly polarized light and the polarization angle (θ) of the plane of polarization:

$$R(\alpha) = \frac{I_O/I_E - 1}{I_O/I_E + 1} = P\cos(2\theta - 4\alpha) \tag{1}$$

Here, (I_O) and (I_E) represent, respectively, the intensities of the ordinary and extraordinary beams, and, α is the angle which the retarder makes with north-south direction.

For calibration of polarization angle zero-point, we observed highly polarized standard stars, and the results are given in Table 2. Both the program and the standard stars were observed during the same night. The obtained values of polarization and position angles for standard polarised stars are in good agreement with Schmidt et al. (1992). To estimate the value of instrumental polarization, unpolarised standard stars were observed. These measurements show that the instrumental polarization is below 0.1 per cent in all pass bands (see Table 2 and also Rautela et al. 2004; Medhi et al. 2007, 2008; Pandey et al. 2009; Eswaraiah et al. 2011, Patel et al. 2013). The instrumental polarization was then applied to all measurements.

3 Studies of the orbital period

3.1 Period analysis

The CLEAN algorithm (Roberts et al. 1987) was used to derive the orbital period of the stars. The clean power spectrum was obtained in each B, V, R and I bands time series data. The power spectrum of V band data is shown in Figure 2(a) for FZ Ori. The peak frequency occured at $\sim 5\ \mathrm{d}^{-1}$ in each filter. The light curve of an eclipsing binary can be represented by two sine waves, therefore multiplying the period ($= 1/\text{frequency}$) by 2 gives appropriate orbital period of the binary system. The mean value of period of the FZ Ori using the CLEAN algorithms was derived to be 0.39998 ± 0.00002 d. This value of the orbital period is similar to the period derived by Figer (1983), Le Brogne et al. (1984) and Zasche et al. (2009). The period corresponding to peak frequency in clean power spectrum for the star V407 Peg was derived to be 0.63686 ± 0.00006 d (see Fig. 2(b)), which is similar to the period derived by the previous authors as Zasche (2011) and Deb and Singh (2011). In the CLEANed power spectrum of LP UMa the maximum power occured at frequency $\sim 6.45386\ \mathrm{d}^{-1}$ (see Fig. 2(c)). The corresponding period was derived to be 0.309892 ± 0.000016 d. This value of the orbital period is similar to the period derived by Csizmadia et al. (2003).

3.2 $O-C$ analysis

3.2.1 FZ Ori

The light minima timings were derived by using Kwee and van Woerden's (1956) method. We have derived 10 timings of minima using our quasi-simultaneous B, V, R and I broad bands observations and 12 timings of minima using All Sky Automated Survey (ASAS; Pojmanski 2002) data (see Table 3). However, 195 timings of minima were collected from the world-wide[2] database of Paschke and Brat

[2] http://var.astro.cz/ocgate/.

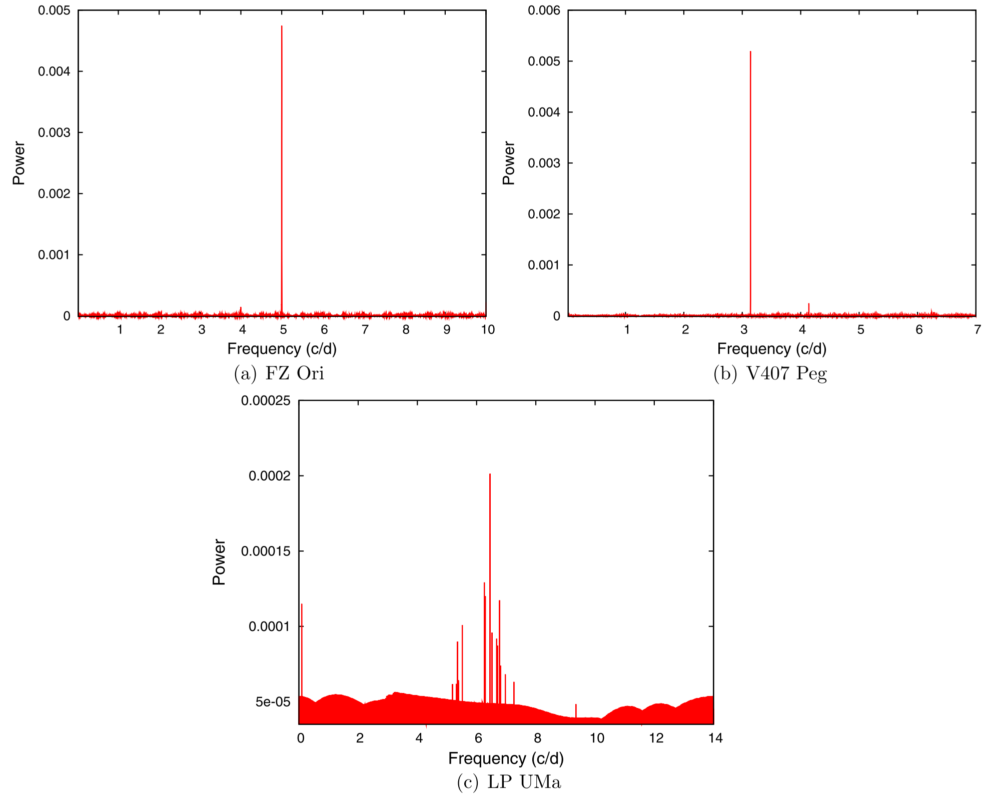

Fig. 2 Cleaned power spectra of (**a**) FZ Ori, (**b**) V407 Peg and (**c**) LP UMa (the most dominant peak in the spectra occurs to ∼5.0 (d^{-1}), ∼3.1404 (d^{-1}) and ∼6.45386 (d^{-1}) for the FZ Ori, V407 Peg and LP UMa binary systems, respectively)

Table 3 Times of light minima of FZ Ori, V407 Peg and LP UMa

HJD-2400000+	Type[a]	Method[b]	Filter	HJD-2400000+	Type[a]	Method[b]	Filter
FZ Ori				V407 Peg			
Observed				Observed			
54878.2435	s	ccd	*BVRI*	55140.1054	p	ccd	*RI*
54880.2497	s	ccd	*BVRI*	55144.2463	s	ccd	*UBVRI*
54886.2333	s	ccd	*BVRI*	55541.0398	s	ccd	*UBVR*
55143.4221	s	ccd	*BVRI*	55903.1023	p	ccd	*BVRI*
55163.4249	s	ccd	*BVRI*	ASAS			
55164.4266	p	ccd	*BVRI*	52812.9352	p	ccd	*V*
55165.4329	s	ccd	*RI*	52918.6604	p	ccd	*V*
55254.2218	s	ccd	*BVRI*	52992.5385	p	ccd	*V*
55257.2165	p	ccd	*BVRI*	53273.7092	s	ccd	*V*
55258.2229	s	ccd	*BV*	54305.8004	p	ccd	*V*
ASAS				54385.7193	s	ccd	*V*
52502.9151	p	ccd	*V*				
52734.5074	p	ccd	*V*	LP UMa			
52745.5055	s	ccd	*V*	Observed			
52884.9031	p	ccd	*V*	55311.1819	p	ccd	*BVRI*
52993.6967	p	ccd	*V*	55312.2515	s	ccd	*BVRI*
53113.4959	s	ccd	*V*	55342.1710	p	ccd	*BVRI*
53626.8773	p	ccd	*V*	55679.1827	s	ccd	*BVRI*
54230.4542	p	ccd	*V*				
54373.8496	s	ccd	*V*				
54392.8484	p	ccd	*V*				
54398.8486	p	ccd	*V*				
54459.6454	p	ccd	*V*				

[a]Type: p = primary minimum time, s = secondary minimum time

[b]Method: ccd = charge-coupled device

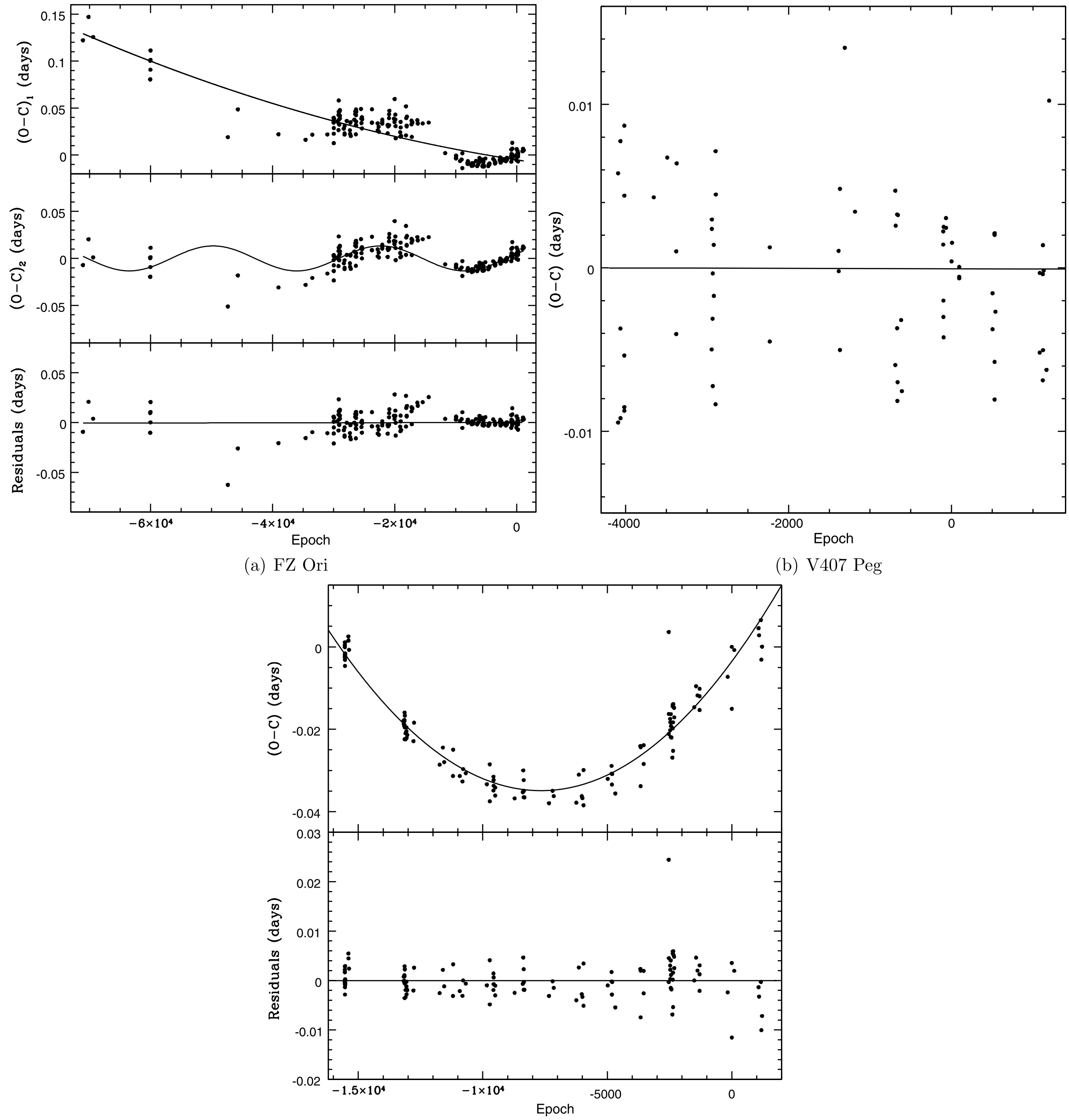

(a) FZ Ori (b) V407 Peg

(c) LP UMa

Fig. 3 (**a**) *The top panel*: $(O-C)_1$ diagram computed using Eq. (2) (the general trend of the $(O-C)_1$ curve reveals a long-term period increase (*dashed line*)). *The middle panel*: the $(O-C)_2$ curve from the parabolic fit and its description by a sinusoidal equation (*solid line*). *The bottom panel*: residuals from Eq. (3)(**b**) $O-C$ residuals from the observed timings of minimum light of V407 Peg (the $O-C$ curve is not changing significantly). (**c**) *The upper panel*: $(O-C)$ diagram computed using Eq. (10); (the general trend of the $(O-C)$ curve revealing a long-term period increase and its description by a quadratic equation (*solid line*)). *The lower panel*: residuals from the parabolic fit of Eq. (11)

(2006) leading total 217 timings of minima over 79 years. From the present photometry the ephemeris of FZ Ori was determined as

$$Min.I\,(HJD) = 2455164.4267(32) + 0^d.3999860(2) \times E \tag{2}$$

Here and onwards the numbers given in parentheses represent the probable errors and are expressed in terms of the last quoted digits. The variation of $O-C$ residuals is shown in the top panel of Fig. 3(a). As seen from the figure the parabolic distribution of the $(O-C)$ vs epoch diagram indicates a long time change in the orbital period. Therefore, we fit the second order polynomial to the data; shown by a dashed line in the top panel of Fig. 3(a). The residuals from second order polynomial fit, $(O-C)_1$, is shown in the middle panel of Fig. 3(a). It is noticed that there is still another change, which seemingly may be sinusoidal. The continuous curve in the middle panel of Fig. 3(a) shows the best sinusoidal fit. The residuals of the sinusoidal fit is shown in the bottom panel of Fig. 3(a), indicating no significant variation. The combined quadratic and sinusoidal fit for the observed data yields

$$\begin{aligned} O-C = {} & -0.0051(\pm 0.0015) - (1.0 \pm 0.1) \times 10^{-6} \times E \\ & + (1.25 \pm 0.24) \times 10^{-11} \times E^2 \\ & + 0.0133(\pm 0.0011) \sin\big[(2.288 \pm 0.039) \times 10^{-4} \\ & \times E + 0.388(\pm 0.091)\big]. \end{aligned} \tag{3}$$

Using the coefficient of square term the rate of change of period (dP/dt) was found to be 2.28×10^{-8} d yr^{-1} (see Dryomova and Svechnikov 2006). The corresponding rate of change of period per cycle (dP/dE) was found to be 2.5×10^{-11} d cycle^{-1}, which is equivalent to a period increase of 0.2 s century^{-1}. The positive sign in the rate of change of period indicates that the period is increased over the course of observations. In the case of conservative mass transfer, this would be caused by a continuously increasing mass flow from the smaller to the larger component of the binary. As the two components of FZ Ori are in a state of over-contact, we take the most likely cause of the period changes as the transfer of mass between the components. The amount of mass transfer, dm is related to the change in period, dP, for a system of total mass, M via (see Coughlin et al. 2008; Yang and Liu 2003)

$$\frac{dm}{dt} = \frac{Mq}{3P(1-q^2)} \frac{dP}{dt} \tag{4}$$

Employing $M = 2.17 M_\odot$ and $q = 0.86 \pm 0.03$; the results transported from Sect. 6, we determine mass transfer rate between the components of FZ Ori to be $1.36 \times 10^{-7} M_\odot$ yr^{-1}. The rate of change of mass ratio (dq/dt) is related with dP/dt via:

$$\frac{dq}{dt} = -\frac{q(1+q)}{3P(1-q)} \frac{dP}{dt} \tag{5}$$

(see Yang and Liu 2003). Employing this relation we have obtained the value of dq/dt to be -2.17×10^{-7} yr^{-1}.

The cyclic variation could be due to either from the magnetic activity of one or both components (Applegate 1992), or the presence of tertiary companion known as LITE (LIght-Time Effect; Irwin 1952, 1959). The amplitude of period oscillations can be determined by using the following relation given by Rovithis-Livaniou et al. (2000),

$$\Delta P = \sqrt{2\big[1 - \cos(2\pi P/P_3)\big]} \times A, \tag{6}$$

where P_3 is orbital period of the third body and A is semi-amplitude of $O-C$ oscillations. P and P_3 are expressed in Years. The orbital period of the third body, P_3 ($= 2\pi P/\omega$; $\omega = 2.288 \pm 0.039 \times 10^{-4}$) is calculated to be 30.1 years. The amplitude of the period oscillation is computed to be $\Delta P = 3.03 \times 10^{-6}$ d leading to the rate of the period variation to be $\Delta P/P = 7.57 \times 10^{-6}$. In order to reproduce this cyclic change, the required variation of the quadruple momentum ΔQ can be calculated using the following relation due to Lanza and Rodonò (2002) and Svechnikov and Kuznetsovs (1990).

$$\frac{\Delta P}{P} = -9 \frac{\Delta Q}{M_{1,2} a^2}, \tag{7}$$

where $a = 2.96 R_\odot$ is separation between the component and $M_{1,2}$ is mass of individual component.

We first determine the total mass ($M_1 + M_2$), using Kepler's third law, to be $2.17 M_\odot$. Now we employ the value of q as 0.86 ± 0.03, obtained later (in Sect. 6) and obtain masses of the primary and the secondary components of FZ Ori to be $1.17 M_\odot$ and $1.0 M_\odot$, respectively. Making use of these values in Eq. (7), the ΔQ has been derived to be 0.83×10^{50} g cm^2 and 0.71×10^{50} g cm^2 for primary and secondary components of FZ Ori, respectively. These values of quadruple momentum are smaller than the typical value of 10^{51}–10^{52} g cm^2 known for close binaries (Lanza and Rodonò 1999), suggesting, that the magnetic mechanism may not suffice to explain the cyclical period variation. Hence we are in favour of the other explanation for the cyclic period variation arising due to the light-time effect via the presence of a third body, with a semi-amplitude of the $O-C$ oscillations. We discuss in the following about an estimate of the mass M_3 of the third body. We first use the relation $a_{12} \sin i' = A \times c$, where i' is the inclination of the orbit of the third component and c is the speed of light, and obtain the value of $a_{12} \sin i'$ to be 2.30 AU. Now the mass function [$f(M_3)$] for the third body is computed using the following well known relation,

$$f(M_3) = \frac{4\pi^2}{GP_3^2} \times \big(a_{12} \sin i'\big)^3 = \frac{(M_3 \sin i')^3}{(M_1 + M_2 + M_3)^2} \tag{8}$$

where M_1, M_2, and M_3 are the masses of the eclipsing pair and the third companion, respectively, and G is the gravitational constant and we obtain it to be $0.014 M_\odot$. Assuming that the third body is coplanar to the orbit of the eclipsing pair (i.e., $i\prime = i = 57.8 \pm 0.2$ degree), the value of the lowest mass of the third body was calculated to be $M_3 = 0.56 M_\odot$.

3.2.2 V407 Peg

The ephemeris of V407 Peg have been derived as

$$Min.I(HJD) = 2455140.10540(87) + 0^d.6368840(4) \times E \tag{9}$$

We derive the timings of the 4 minima using our quasi-simultaneous B, V, R and I broad bands observations and 6 timings of minima using ASAS data. These timings of minima are given in Table 3. Including the timings of minima from Paschke and Brat (2006) we have a collection of total 74 timings of minima over a span of 9 years. We make use of this data set for $O-C$ analysis. The variation of $O-C$ residuals, against the epoch number is shown in Fig. 3(b). As seen from this figure the $O-C$ is constant over the course of observations, indicating no change in the orbital period during 9 years of its observations.

3.2.3 LP UMa

We, making use of our observations, have determined the ephemeris of LP UMa as

$$Min.I\,(HJD) = 2455311.18194(211) + 0^d.3098980(2) \times E \tag{10}$$

The timings of minima derived from present photometry are given in Table 3. Total 118 timings of minima over a span of 14 years were found using the world-wide database of minima timings of Paschke and Brat (2006). The residuals of $O-C$ curve as a function of epoch number is plotted in Fig. 3(c). The $O-C$ vs epoch diagram distribution is parabolic, similar to FZ Ori. The best fit second order polynomial is shown by continuous line in the upper panel of Fig. 3(c). The residuals from polynomial fit is shown in the lower panel of Fig. 3(c), which reveal that there is no significant variation. The quadratic fit for the observed data is obtained as:

$$\begin{aligned} O-C = {} & -0.0036(\pm 0.0008) + (8.2 \pm 0.3) \times 10^{-6} \times E \\ & + (5.3 \pm 0.2) \times 10^{-10} \times E^2 \end{aligned} \tag{11}$$

Using the similar method as used for FZ Ori system, the period of LP UMa has been determined and is found to be increasing with rate of $1.25 \times 10^{-6}\ \mathrm{d\,yr^{-1}}$ equivalent to $1.06 \times 10^{-9}\ \mathrm{d\,cycle^{-1}}$. This indicates that the period has increased by $10.8\ \mathrm{s\,century^{-1}}$.

4 Light curves from present observations

The phase folded light curves of FZ Ori, V407 Peg and LP UMa are shown in Figs. 6(a), 6(b) and 6(c), respectively. The features of the light curves seen are typical of W UMa type systems. The primary and secondary minima of FZ Ori and LP UMa are found to be rounded, whereas, the light curves of V407 Peg present a flatter bottom at the secondary eclipse and inclined and distorted primary one. The secondary eclipse is slightly deeper than the primary one. The corresponding difference between the primary and secondary minima is found to be in the range 0.01–0.02 magnitudes for FZ Ori. The difference is well within 1σ level. But for V407 Peg and LP UMa, the primary eclipse is deeper than the secondary one with the respective differences in B, V, R and I bands, in range of 0.07–0.1 magnitudes and 0.06–0.08 magnitudes. The differences of magnitudes between the primary maximum ($\phi = 0.25$) and the minimum ($\phi = 0.0$) in B, V, R, and I bands are about 0.40–0.43 for FZ Ori, 0.47–0.54 for V407 Peg and 0.20–0.23 for LP UMa, respectively. However, differences between the secondary maximum ($\phi = 0.75$) and the minimum ($\phi = 0.50$) in B, V, R, and I bands range from 0.37–0.41 magnitudes for FZ Ori, 0.35–0.38 magnitudes for V407 Peg and 0.15–0.20 magnitudes for LP UMa. Such differences in this range are also found for additional U band data of V407 Peg. Similar differences between maximum and minimum have also been observed for FZ Ori by El-Bassuny Alawy (1993), Rukmini et al. (2001) and Byboth et al. (2004), for V407 Peg by Deb and Singh (2011), Zasche (2011) and Lee et al. (2014) and for LP UMa by Csizmadia et al. (2003).

In the W UMa systems, both the stars are very close to each other, so, there is a continuous variation outside of the eclipses as well. Because of this, the stars will experience gravitational distortion and heating effects. The observed light curves of FZ Ori, V407 Peg and LP UMa are asymmetric. The primary maximum of FZ Ori and of V407 Peg are brighter than the secondary maximum, whereas the secondary maximum of LP UMa is brighter than the primary maximum. The magnitude differences between the phases 0.25 and 0.75 were found to be in the range of 0.02–0.05 magnitudes in all bands for all the binaries. These may be due to stellar activity such as starspots caused either by a magnetic property or by impact of mass transfer between the component stars.

5 Estimation of basic parameters

The colour of the binary system is calculated using period-colour relation (Wang 1994):

$$(B-V)_0 = 0.062 - 1.310 \log P \tag{12}$$

where orbital period P is in days. This relation yields the intrinsic colours $[(B-V)_0]$ to be 0.583, 0.319 and 0.729 mag for the FZ Ori, V407 Peg and LP UMa stars systems, respectively. The effective temperature of primary component is now computed by using the following relation (Wang 1994):

$$(B-V)_0 = \frac{3.970 - \log T_{\mathrm{eff}}}{0.310} \tag{13}$$

The values of T_{eff} for primary components of FZ Ori, V407 Peg and LP UMa are calculated to be 6030 K, 7394 K and

5570 K, respectively. The infrared colour suffers negligible reddening, therefore, is a good tracer for spectral type. The $(J-K)$ colour indices for FZ Ori, V407 Peg and LP UMa, using 2MASS catalogue (Cutri et al. 2003) turns out to be 0.342 ± 0.035, 0.181 ± 0.033 and 0.400 ± 0.034, respectively. These values when used in the colour-temperature calibration of Cox (2000) yield temperatures and corresponding spectral types of 5940 K and $G0$, 7300 K and F0V, and 5794 K and $G5V$ for the primary components of the FZ Ori, V407 Peg and LP UMa, respectively.

Rucinski and Duerbeck (1997) have obtained a calibration of absolute magnitude (M_V) of W UMa-type systems in terms of their $(B-V)_0$ colour and period as

$$M_v = -4.44 \log P + 3.02(B-V)_0 + 0.12 \qquad (14)$$

Employing this calibration we obtain M_V of FZ Ori to be 3.65 mag. Now taking the visual magnitude (V) as 10.53 and assuming the negligible reddening, the distance modulus of FZ Ori is calculated to be 6.88 mag, leading to a distance of 237.68 pc. Using the parallax of V407 Peg as 3.06 ± 0.38 mas (Bilir et al. 2005), the distance of V407 Peg turns out to be 327 ± 41 pc. Using Equation (14), we find the value of M_V to be 4.06 mag for the LP UMa binary system, which when adopted with its the visual magnitude (V) as 12.53, results its distance modulus to be 8.47 mag. This leads to a distance of 493.40 pc for LP UMa binary system.

6 Light curve modeling and photometric solutions

We have modeled multi-band light curves of FZ Ori, V407 Peg and LP UMa using WD code (Wilson and Devinney 1971), implemented in PHOEBE[3] (Prša and Zwitter 2005). It is a modified package of the widely used WD program for deriving the geometrical and physical parameters of the eclipsing binary stars. In the WD code, some of the parameters need to be fixed and the convergence of the solutions are obtained using the methods of multiple-subsets (Wilson and Biermann 1976). Since most of the W UMa binaries are contact binaries, therefore, mode-3 of WD code is the most suitable for the light curve analysis. However, we start with mode-2 (detached binary) and achieve the convergence of the solution and thereafter go to mode-3 (over-contact configuration) for the final convergence. In the light curve analysis using the WD code, star 1 is the one eclipsed at primary minimum and star 2 is the other eclipsed at secondary minimum.

The temperature of the star 1, the mass ratio (q), the bolometric albedos ($A_1 = A_2 = 0.5$ for stars with convective envelopes and 1.0 for radiative envelopes; Ruciński 1969) and gravity darkening coefficients ($g_1 = g_2 = 0.32$ for convective envelopes and 1.0 for radiative envelopes; Lucy 1967) were the input parameters for all binaries (see Table 4). These parameters were kept fixed to obtain exact solution. The bolometric (x_{1bol}, y_{1bol}, x_{2bol}, y_{2bol}) and monochromatic (x_1, x_2, y_1, y_2) limb darkening coefficients of the components are interpolated using Logarithmic law from van Hamme (1993) tables. The adjustable parameters were the temperature of the star 2 (T_2), orbital inclination (i), the surface potentials of both components (Ω_1 and Ω_2; $\Omega_1 = \Omega_2$ for contact binaries), and monochromatic luminosity of star 1 (L_1). During the photometric solution, a third object, with light l_3 has also been taken as an adjustable parameter in order to get better fit of the light curves. The third light l_3 is in the unit of total light as implemented in PHOEBE. However, determination of third light from the photometric light curve modeling sometimes affects the orbital inclination and amplitude of the light curve. However, evidence of a third light was found in the case of FZ Ori (see Section 3), hence we can not ignore light curve modeling.

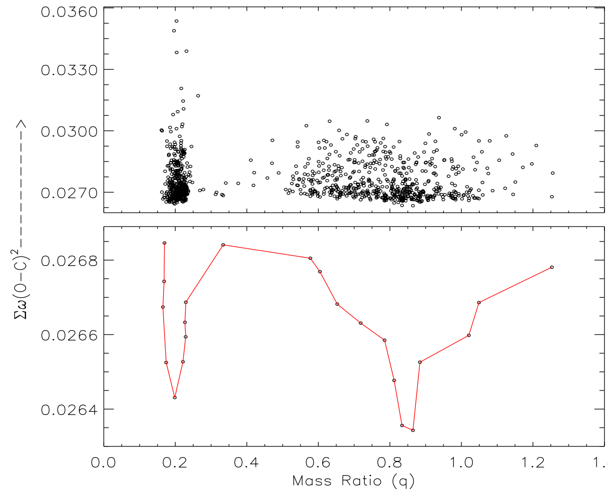

Fig. 4 *The upper panel*: plot of the sum of weighted-square deviations, $\sum \omega_i (O-C)^2$ versus mass ratio, q of FZ Ori for several iterations. *The lower panel*: variation of q with $\sum \omega_i (O-C)^2$ for small range

We performed test solutions at the outset by using a q-search method. In the q-search method, the test solutions have been obtained for several of the assumed values of the mass ratio, q $(= M_2/M_1)$ starting from 0.1 to 1.3 in steps of 0.1 for achieving a reliable mass ratio of the system. Also, assuming that the system is a detached binary, the differential corrections (dc) have been started from the mode-2 and thereafter rapidly ran into the mode-3 (contact configuration). The behavior of the resulting sum of weighted-square deviations, $\sum \omega_i (O-C)^2$ versus q is plotted in Fig. 4. The upper panel of Fig. 4 is showing the variation of $\sum \omega_i (O-C)^2$ with q for several iterations. The minimum of sum of weighted-square deviations, obtained after several iterations, and their corresponding mass ratio

[3] http://phoebe.fiz.uni-lj.si/.

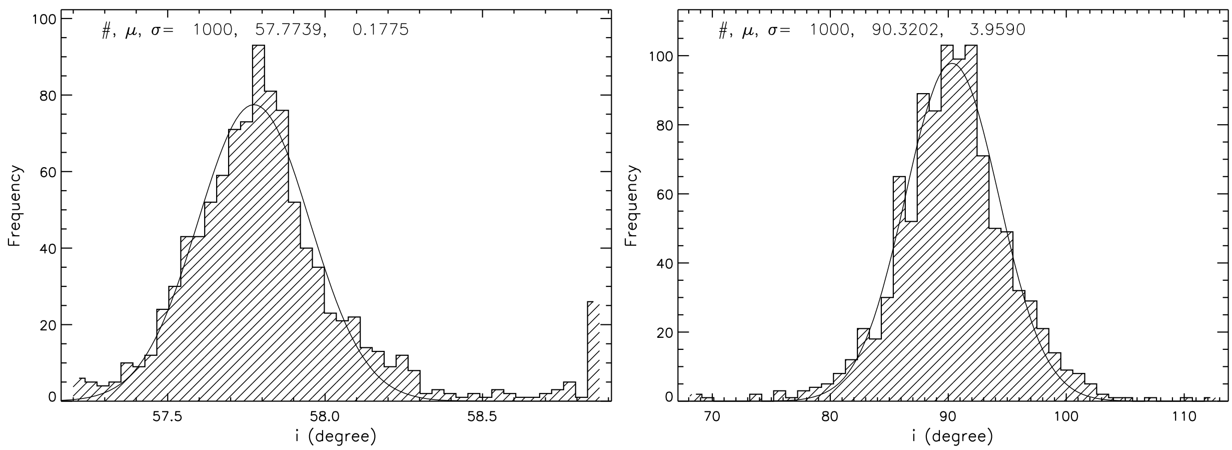

(a) FZ Ori (b) V407 Peg

Fig. 5 Histograms of the results obtained using the Monte Carlo parameter scan for the parameters fit of inclination in the contact mode with PHOEBE for the (**a**) FZ Ori and (**b**) V407 Peg

values determined from the upper panel are plotted in the lower panel of Fig. 4. The purpose of this plot is of checking the variation of the mass ratio with sum of weighted-square deviations for small range. Now it is easy to see from the plot that $\sum \omega_i (O-C)^2$ is minimum at $q = 0.86$. To check this value of the mass ratio, we performed a differential correction once again starting from the dc solutions at $q = 0.86$ and by considering the mass ratio as freely adjustable parameters along with the other adjustable parameters. The final solution with converged mass ratio, $q = 0.86 \pm 0.03$ has been obtained. The spectroscopic mass ratio (q_{spec}) of 0.256 ± 0.006 (Rucinski et al. 2008) for V407 Peg has been adopted during the modeling of the light curves. While, in case of LP UMa, we have used the mass ratio, $q = 0.886 \pm 0.015$ (Csizmadia et al. 2003) for modeling of the light curves. During the modeling of the light curves, we find that the theoretical light curves do not fit very well with the observed ones, especially around the maxima. Therefore, the spot models were adopted to fit the observed light curves. We consider the possible spot models of hot / cool spots on the primary/secondary component. We then carry forth by iteration, allowing the spot latitude (ranging from 0° at the north pole to 180° at the south pole), the longitude (ranging from 0° to 360°, with 0° at the inner Lagrangian point, 180° at the back end, and increasing in the direction of rotation), the angular radius (where 90° covers exactly half the star), the temperature factor (the ratio of the spot temperature to the underlying surface temperature), and temperature of secondary (T_2) to vary until a satisfactory fit was found i.e. until any further corrections are less than the errors. At this point, having obtained both orbital and spot parameters, we solve it further for a final solution for folded un-binned light curve, allowing all previously mentioned parameters to vary, once again until any further corrections were less than the errors. It turns out that placing spots on the primary components of FZ Ori, V407 Peg and LP UMa were found to be better than the spot on the secondary. Therefore, we take these as our final (best fit) solutions that corresponds to the minimum sum of the square of the residuals value among them. The best fit theoretical light curves (solid lines) along with the observed light curves of FZ Ori, V407 Peg and LP UMa are shown in Figs. 6(a), 6(b) and 6(c), respectively. The corresponding geometric configurations with a bright spot on the primary components of FZ Ori and V407 Peg, and cool spot on this component of LP UMa are shown in Fig. 7.

The spot solutions included in the WD code can easily be fitted to the whole light curve but poses a serious problem regarding uniqueness of the solution (Maceroni and van't Veer 1993) unless other means of investigation such as Doppler Imaging techniques are applied (Maceroni et al. 1994). The WD's differential correction (dc) minimization program yields the values of the fitting parameters as well as the formal statistical errors associated with each of them. We perform the Monte Carlo parameter scan (heuristic scan) around the best solution making use of the PHOEBE's scripter capability (Bonanos 2009) with a view to explore the values, errors and stability of the solutions. The WD's (dc) minimization program was run 1000 times, updating each time the input parameter values for the next iteration. We obtain the final values for the parameters as the mean of the parameters resulted in various iterations. The errors on these parameters were derived by determining the standard deviations. Figure 5 shows the histogram of the result obtained using the heuristic scan method for the orbital inclination, i in the contact mode with PHOEBE for the FZ Ori and V407 Peg.

In case of our target contact binaries, the light curve synthesis solutions from the present data indicate the need of a third light. The presence of third light shows a tight correlation with the inclination angle and the mass ratio. However,

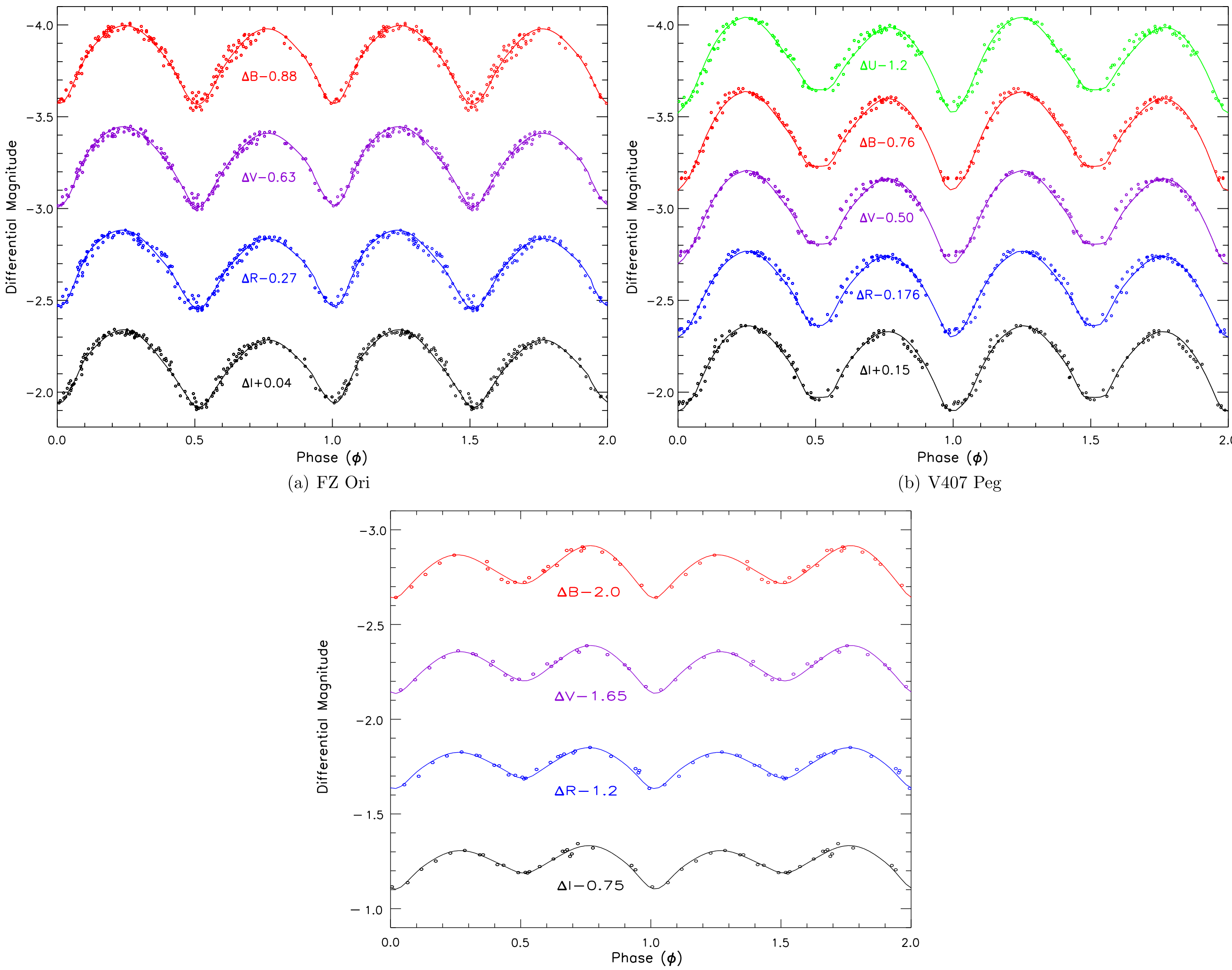

(a) FZ Ori

(b) V407 Peg

(c) LP UMa

Fig. 6 Phased light curves of the (**a**) FZ Ori, (**b**) V407 Peg and (**c**) LP UMa in B, V, R and I broad bands along with the phased light curve in U band only for V407 Peg (*Open circles* denote the observational data points. *The continuous line* is the synthetic light curves computed from the WD light curve modeling technique considering the case as presence of spot on the primary component of FZ Ori, V407 Peg and LP UMa, respectively)

in the light curve modeling of the FZ Ori and V407 Peg the mass ratios were kept fixed, therefore the third light is highly correlated with the orbital inclination angles as shown in Figs. 5(a) and 5(b), respectively. During light curve modeling of the LP UMa, the inclination angle and mass ratio values were adopted from previous study due to lack of huge data points. Precession of the orbital plane and an apsidal motion of the close binaries could be due to the third body orbiting the binary system. In eclipsing binaries, the change in orbital inclinations and consequently, change in the photometric amplitude of the eclipses are due to the precession of the orbital plane.

The best fit parameters of FZ Ori, V407 Peg and LP UMa are given in the Table 4. The fractional stellar radii $r_{1,2}$ obtained from the light curve modeling are normalized to the semi-major axis of the binary system, i.e., $r_{1,2} = R_{1,2}/a$, where a and R are the semi-major axis and the component radii, respectively. The component radius for each star (in solar radius units) may be determined using the above relation, in which r is taken as the geometrical mean of the r-pole, r-side and r-back radii. For V407 Peg the value of a is calculated using i and P from the present-study and radial velocity amplitude from Rucinski et al. (2008). However, for LP UMa a was taken from Csizmadia et al. (2003). From the modeling of the light curves, the temperature difference between the primary and secondary components of FZ Ori, V407 Peg and LP UMa systems were found to be ∼43 K, ∼812 K and ∼873 K, respectively.

We determine the absolute physical parameters (mass, radius and luminosity) of the components of the binaries systems based on the results of the light curve solution. The luminosity of the star was calculated using the temperature

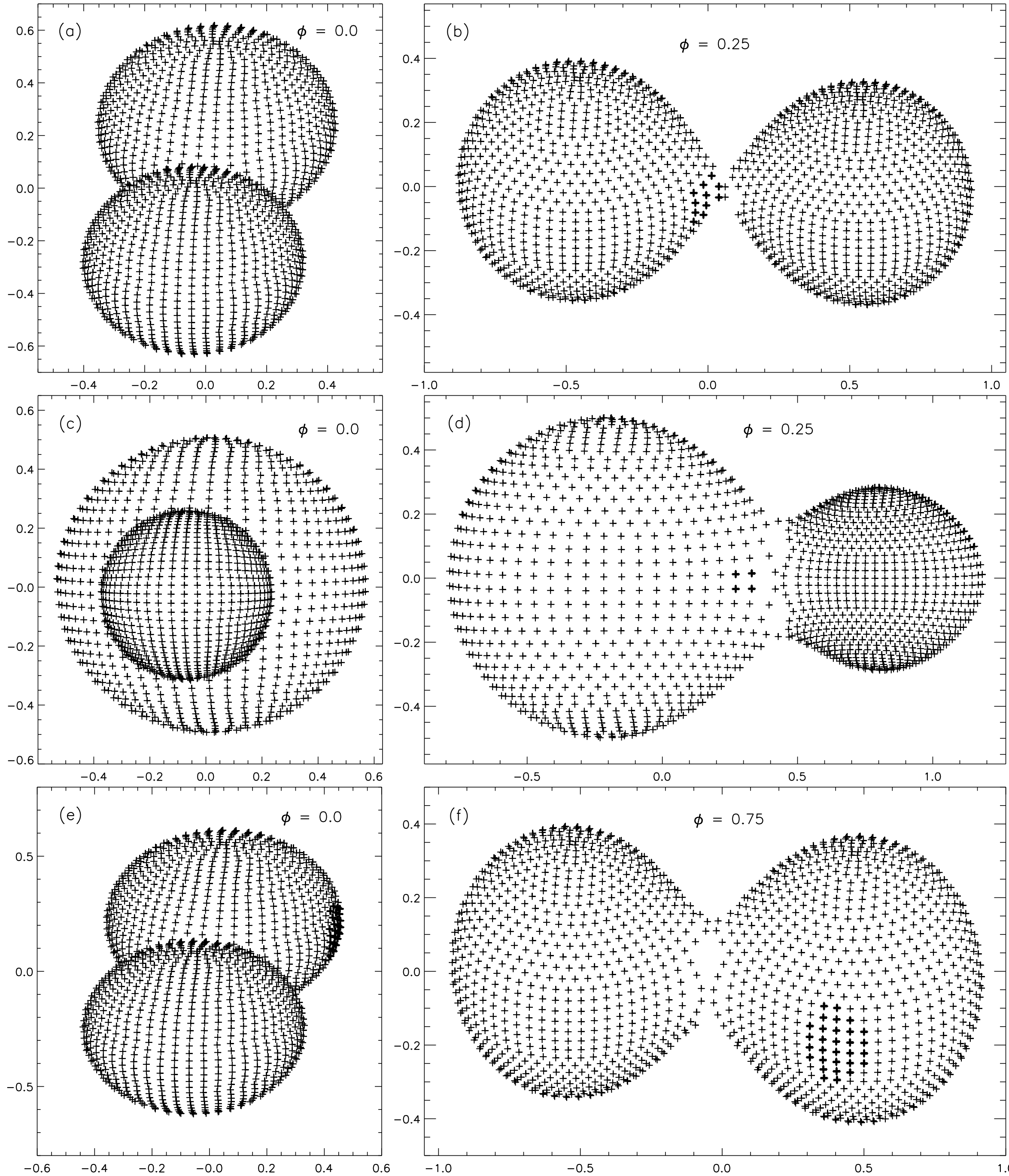

Fig. 7 Geometric configurations (**a**) and (**b**) FZ Ori, (**c**) and (**d**) V407 Peg, and (**e**) and (**f**) LP UMa generated by PHOEBE showing spots on the primary component

and radius of each of the individual components. Table 5 lists the results regarding the physical parameters of the individual components of the FZ Ori, V407 Peg and LP UMa systems.

The eclipsing binaries are classified into contact, semi-detached and detached binaries according to fill factor (f) as $0 < f < 1$, $f = 0$ and $f < 0$, respectively. The fill-out factor (f) is defined as:

$$f = \frac{\Omega_{in} - \Omega_{1,2}}{\Omega_{in} - \Omega_{out}} \tag{15}$$

where Ω_{in} and Ω_{out}, and $\Omega_{1,2}$ are the inner and outer Lagrangian surface potentials, and surface potentials of the star 1 and 2, respectively. In case of contact binaries surface potentials of primary and secondary are equal to the surface

Table 4 Photometric solutions obtained from the light curve modeling of the FZ Ori, V407 Peg and LP UMa

Parameters	Symbol	FZ Ori	V407 Peg	LP UMa
Mass ratio (M_2/M_1)	q	0.86 ± 0.03	0.256 ± 0.006	0.886 ± 0.015
Orbital inclination [°]	i	57.77 ± 0.18	90.32 ± 3.96	62.84 ± 1.35
Relative luminosity of star 1 (U)	$[L_1/(L_1+L_2)]$	…	0.877	…
(B)	$[L_1/(L_1+L_2)]$	0.534	0.852	0.749
(V)	$[L_1/(L_1+L_2)]$	0.532	0.830	0.717
(R)	$[L_1/(L_1+L_2)]$	0.533	0.802	0.691
(I)	$[L_1/(L_1+L_2)]$	0.526	0.798	0.667
Monochromatic ld coefficients (U)	$(x_{1U} = x_{2U})$	…	0.773	…
	$(y_{1U} = y_{2U})$	…	0.305	…
(B)	$(x_{1B} = x_{2B})$	0.774	0.803	0.769
	$(y_{1B} = y_{2B})$	0.159	0.294	0.171
(V)	$(x_{1V} = x_{2V})$	0.731	0.698	0.732
	$(y_{1V} = y_{2V})$	0.065	0.285	0.051
(R)	$(x_{1R} = x_{2R})$	0.644	0.590	0.650
	$(y_{1R} = y_{2R})$	0.170	0.276	0.164
(I)	$(x_{1I} = x_{2I})$	0.568	0.492	0.572
	$(y_{1I} = y_{2I})$	0.207	0.259	0.202
Bolometric ld coefficients	$(x_{1bol} = x_{2bol})$	0.627	0.650	0.622
	$(y_{1bol} = y_{2bol})$	0.098	0.238	0.099
Third light (U)	l_{3U}	…	0.23 ± 0.03	…
(B)	l_{3B}	0.71 ± 0.01	0.20 ± 0.02	0.46 ± 0.06
(V)	l_{3V}	0.67 ± 0.02	0.20 ± 0.02	0.46 ± 0.07
(R)	l_{3R}	0.61 ± 0.04	0.22 ± 0.01	0.43 ± 0.07
(I)	l_{3I}	0.51 ± 0.03	0.21 ± 0.04	0.45 ± 0.11
Surface Potentials	$(\Omega_1 = \Omega_2)$	3.509 ± 0.002	2.231 ± 0.005	3.496 ± 0.013
Inner contact surface	(Ω_{in})	3.519	2.367	3.562
Outer contact surface	(Ω_{out})	3.039	2.206	3.071
Fill-out factor	f	0.02	0.84	0.14
Effective temperatures	T_1 (K)	5940	7300	5794
	T_2 (K)	5983 ± 16	6504 ± 67	4921 ± 41
Surface albedos (bolometric)	$A_1 = A_2$	0.50	1.0	0.50
Gravity darkening coefficients	$g_1 = g_2$	0.32	1.0	0.32
Synchronicity parameters	$F_1 = F_2$	1.0	1.0	1.0
Relative Radii of components				
(pole)	r_{1pole}	0.3691 ± 0.0004	0.450 ± 0.004	0.383 ± 0.003
	r_{2pole}	0.3439 ± 0.0004	0.286 ± 0.005	0.363 ± 0.003
(side)	r_{1side}	0.3885 ± 0.0005	0.551 ± 0.006	0.406 ± 0.004
	r_{2side}	0.3607 ± 0.0005	0.304 ± 0.006	0.384 ± 0.004
(back)	r_{1back}	0.4191 ± 0.0007	0.588 ± 0.008	0.446 ± 0.006
	r_{2back}	0.3923 ± 0.0007	0.395 ± 0.026	0.425 ± 0.007
Spot parameters				
Spot latitude	$[\phi\ (°)]$	90.0	90.0	90.0
Spot longitude	$[\theta\ (°)]$	349.56	333.0	86.0
Spot radius	$[r_s\ (°)]$	11.01	7.21	17.0
Spot temperature factor	(T_s/T_*)	1.418 ± 0.003	1.83	1.197 ± 0.005
Absolute bolometric magnitudes	M_{bol1}	3.71	1.95 ± 0.09	4.139
	M_{bol2}	3.70	3.49 ± 0.11	4.402
Effective gravity of the components	$\log g_1$ (cgs)	4.38	4.03 ± 0.08	4.221
	$\log g_2$ (cgs)	4.37	3.86 ± 0.30	4.123

Table 5 Absolute parameters obtained from the light curve modeling

Parameters	Symbol	FZ Ori	V407 Peg	LP UMa
Semi-major axis	$[a_{orb}\ (R_\odot)]$	2.96	4.17 ± 0.08	2.170
Total Mass	$(M_1/M_\odot + M_2/M_\odot)$	2.17	2.40 ± 0.10	1.424
Mass function	$f\ (M_\odot)$	1.32	2.40 ± 0.08	1.003
Mass				
Primary	$(M_1/M_\odot)$	1.17	1.91 ± 0.08	0.755
Secondary	$(M_2/M_\odot)$	1.0	0.49 ± 0.06	0.669
Radius				
Primary	$(R_{\star 1}/R_\odot)$	1.16	2.21 ± 0.05	0.894
Secondary	$(R_{\star 2}/R_\odot)$	1.08	1.37 ± 0.06	0.849
Luminosity				
Primary	$(L_1/L_\odot)$	1.50	12.43 ± 0.39	0.807
Secondary	$(L_2/L_\odot)$	1.34	3.01 ± 0.19	0.379

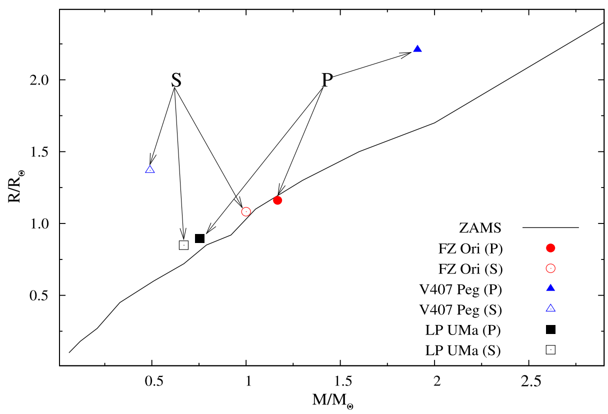

Fig. 8 Location of the primary and secondary components of FZ Ori, V407 Peg and LP UMa on a mass-radius diagram. *The continuous line* shows the zero age main sequence, where P and S represent primary and secondary components of the binaries, respectively.

potential (Ω) of common envelope for the binary system (i.e. $\Omega_1 = \Omega_2 = \Omega$). For semi-detached binaries with the primary and secondary components filling their Roche lobe, $\Omega_1 = \Omega_2 = \Omega_{in}$, respectively. However, for detached binaries $\Omega_{1,2} > \Omega_{in}$. The fill-out factors for the FZ Ori, V407 Peg and LP UMa are obtained to be 0.02, 0.80 and 0.14, respectively indicating the that these are contact binaries.

The computed absolute parameters of FZ Ori, V407 Peg and LP UMa, as reported in Table 5, are used to estimate the evolutionary status of the system by means of the mass-radius diagram, shown in Fig. 8. In this plot, the solid line represents the zero age main sequence (ZAMS) from Schaifers and Voigt (1982). The positions of primary and secondary components of FZ Ori are on ZAMS. However, the position of both components of V407 Peg on the mass-radius diagram are far above the ZAMS. In case of LP UMa, both components are located slightly above the ZAMS. It is evident from the figure that the radius of the primary component approaches to the value for zero age main sequence (ZAMS) stars. It is also noticed from the figure that the mass-radius relation of the secondary is slightly different from that of ZAMS stars, i.e. the secondary component is clearly far above the ZAMS and which is due to the fact that the mass transfer between the components may restructure the secondary and make it over-sized and over-luminous for its mass (see also Webbink 2003; Li et al. 2008).

7 Results of polarimetric observations

The values of Stokes parameters (Q and U) and the degree of polarization (P) in B, V, R and I bands at different orbital phases for FZ Ori and V407 Peg are given Table 7. The variations in the Stokes parameters of FZ Ori and V407 Peg with their orbital phases in the different bands are shown in Fig. 10. The phases of FZ Ori and V407 Peg were computed using the Eqs. (2) and (9), respectively. The polarimetric observations of FZ Ori have been taken during the phases 0.01-0.21 and 0.88-0.99. While, most of the polarimetric observations of V407 Peg were taken during the phase from 0.54 to 0.85. The Stokes parameters appear to be orbital phase dependent. However, due to lack of the full phase coverage, the phase locked variability could not be confirmed. Furthermoer we have not found any defnitiv trend in polarization variation. The mean values of degree of polarization and polarization position angles in B, V, R and I bands, of FZ Ori were calculated to be 0.26 ± 0.03, 0.22 ± 0.02, 0.22 ± 0.03 and 0.22 ± 0.05 per cent & 117 ± 2, 104 ± 2, 74 ± 3 and 86 ± 3 degree, respectively. While for V407 Peg, the mean values of degree of polarization and polarization position angles in B, V, R and I bands, were calculated to be 0.21 ± 0.02, 0.29 ± 0.03, 0.31 ± 0.01 and 0.31 ± 0.04 per cent & 75 ± 2, 61 ± 3, 73 ± 1 and 62 ± 3 degree, respectively.

The interstellar polarization, due to the dust in the interstellar medium (ISM) located between the observer and

Table 6 Stars taken from Heiles (2000) catalog for finding interstellar polarization of FZ Ori

Star's name	$P \pm \epsilon_P$ (%)	Distance (pc)	$\theta \pm \epsilon_\theta$ (°)	Q (%)	U (%)
HD 37958	0.143 ± 0.024	357 ± 79	48.0 ± 4.8	-0.015 ± 0.024	0.142 ± 0.024
HD 37984	0.080 ± 0.032	90 ± 3	46.0 ± 11.3	-0.003 ± 0.032	0.080 ± 0.032
HD 37606	0.150 ± 0.032	394 ± 93	36.0 ± 6.1	0.046 ± 0.032	0.143 ± 0.032
HD 38047	0.138 ± 0.023	218 ± 35	47.0 ± 4.8	-0.010 ± 0.023	0.138 ± 0.023

the star, may also contribute in the observed polarization values of FZ Ori and V407 Peg. Hence, in order to obtain the true value of polarization, it is essential to subtract the component due to the ISM from the observed polarization values. Following Schlegel et al. (1998), the interstellar extinction $[E(B-V)]$ towards the direction of FZ Ori and V407 Peg are 0.539 and 0.067, respectively. The extinction towards the direction of FZ Ori appears to be high, therefore, the polarization due to ISM needs to subtracted from the observed polarization. However, in case of V407 Peg the extinction is very low indicating the negligible polarization due to ISM. Further, the maximum polarization due to ISM can not exceed the empirical upper limit of $9.0E(B-V)$; the maximum polarization towards the direction FZ Ori and V407 Peg was derived to be 5.0 % and 0.6 %, respectively. The contribution to the polarization values due to the foreground ISM at a distance of program stars can be estimated by measuring the polarization values of stars with known distance. In order to derive polarization values due to ISM, we have searched stars within a circular region of radius of 1.5° around FZ Ori, whose both polarization and distance measurements are available in the literature. We found 4 such stars. Their polarization measurements are given in Heiles (2000) catalog. Their distances based on the Hipparcos parallax measurements are available in the catalog by van Leeuwen (2007). Their distances along with their polarization values in V-band are given in Table 6. We have plotted the values of the Q and U Stokes parameters as a function of their distances in Figs. 9(a) and (b). We have derived the Stoke's parameters Q_{ism} and U_{ism} representing the foreground dust component by making a straight line fit to the data points, as shown in Figs. 9(a) and (b). We found the following relations for Q_{ism} and U_{ism}: $Q_{ism} = 10^{-4}.d - 0.027$ and $U_{ism} = 1.9 \times 10^{-4}.d + 0.079$, respectively. Using these relations, we have derived Q_{ism} and U_{ism} for FZ Ori (distance = 237.68 pc) as -0.003 and 0.124, respectively. These values were subtracted from the corresponding Stoke's parameters to get foreground corrected Stokes parameters Q_{in} and U_{in} values. The stars selected from Heiles (2000) catalog have polarization values only in V-band, therefore, we have made corrections only in V-band polarization values. The V-band polarization due to ISM at the distance of FZ Ori is calculated to be 0.124 %. Using Serkowski law (1975), the maximum ISM polarization, of about 0.1 % is found near the V-band (λ 0.55 nm), indicating that the polarization due to ISM at a distance of FZ Ori in B, R and I bands should be less than 0.1 %. The ISM polarization corrected average values of the Stoke's parameters of FZ Ori are found to be -0.147 and -0.119 leading to degree of polarization in V-band to be 0.190 % and the corresponding position angle to be 20°.

The intrinsic polarization can be explained by the scattering of light in a gaseous envelope. Shakhovskoi (1965) had suggested a model envelope to estimate the degree of polarization of the light scattered by the envelope, where the envelope has the shape of a ring lying in the orbital plane of the system and where Thomson scattering is the principal scattering mechanism. It is well known that many close binary systems contain gaseous streams and envelopes formed through ejection of the material from the atmospheres of one or both components. If such an envelope is not spherically symmetric, for example, if the gas is concentrated towards the orbital plane, scattering of light in the envelope may generate a polarization that would be observed in the integrated light of the system. In W UMa-type binaries one component fills its Roche lobe and loose mass through the inner Lagrangian point in the form of gas stream and latter it being located in the plane of orbit. The polarization arises at light scattering of both components on gas streams and the polarization is maximum when the scattering angles approaches to 90°.

8 Discussion and conclusions

We have presented a detailed photometric analyses of eclipsing binaries FZ Ori, V407 Peg and LP UMa. The light curves of these binaries are found to be variable. FZ Ori and V407 Peg display O'Connell effects with the primary maximum brighter than the secondary maximum. While, the light curves of LP UMa show the O'Connell effects with the secondary maximum brighter than the primary maximum. The asymmetric light curves have been explained by the spot model. The slightly variable bright spot on the primary star may hold good to explain light-curve representations for all three systems. The light curves of FZ Ori system show the partial eclipse nature. The slightly higher temperature of the secondary component of FZ Ori system and it's mass ratio value indicate that it is a W-type contact binary. Byboth et al.

Table 7 Results of the Stoke's parameters and degree of polarization observed for FZ Ori and V407 Peg in B, V, R and I bands

JD	Phase	Filter	$Q \pm \epsilon_Q$ (%)	$U \pm \epsilon_U$ (%)	$P \pm \epsilon_P$ (%)	JD	Phase	Filter	$Q \pm \epsilon_Q$ (%)	$U \pm \epsilon_U$ (%)	$P \pm \epsilon_P$ (%)
FZ Ori						V407 Peg					
2455548.36613	0.8822	B	−0.01 ± 0.03	0.13 ± 0.04	0.13 ± 0.04	2455485.06619	0.6383	B	−0.10 ± 0.01	0.04 ± 0.01	0.11 ± 0.01
2455548.39498	0.9543	B	0.20 ± 0.16	−0.35 ± 0.17	0.40 ± 0.18	2455485.08147	0.6623	V	−0.29 ± 0.01	0.19 ± 0.02	0.35 ± 0.01
2455548.42164	0.0210	B	0.22 ± 0.04	−0.19 ± 0.04	0.29 ± 0.04	2455485.10103	0.6930	R	−0.21 ± 0.05	0.17 ± 0.04	0.27 ± 0.05
2455548.44597	0.0818	B	0.31 ± 0.21	−0.01 ± 0.17	0.31 ± 0.21	2455485.11399	0.7134	I	−0.21 ± 0.18	0.03 ± 0.13	0.21 ± 0.18
2455548.37366	0.9010	V	−0.22 ± 0.01	−0.12 ± 0.01	0.25 ± 0.01	2455486.28149	0.5466	I	−0.07 ± 0.07	0.38 ± 0.07	0.39 ± 0.07
2455548.40429	0.9776	V	−0.02 ± 0.01	0.11 ± 0.01	0.11 ± 0.01	2455527.20583	0.8037	B	−0.30 ± 0.05	0.31 ± 0.05	0.43 ± 0.05
2455548.42922	0.0399	V	−0.13 ± 0.05	0.19 ± 0.06	0.23 ± 0.06	2455527.19191	0.7818	V	−0.12 ± 0.11	0.12 ± 0.11	0.17 ± 0.13
2455548.45310	0.0996	V	−0.16 ± 0.11	0.17 ± 0.11	0.23 ± 0.12	2455527.21978	0.8256	R	−0.25 ± 0.01	−0.03 ± 0.01	0.25 ± 0.01
2455548.37963	0.9159	R	−0.15 ± 0.14	−0.34 ± 0.16	0.37 ± 0.16	2455548.09932	0.6095	B	−0.13 ± 0.03	0.25 ± 0.03	0.28 ± 0.03
2455548.40949	0.9906	R	−0.25 ± 0.01	0.22 ± 0.02	0.33 ± 0.01	2455548.12407	0.6483	B	−0.10 ± 0.04	0.14 ± 0.05	0.17 ± 0.05
2455548.43424	0.0525	R	−0.08 ± 0.05	0.09 ± 0.05	0.12 ± 0.06	2455548.14802	0.6859	B	−0.12 ± 0.04	−0.02 ± 0.03	0.12 ± 0.04
2455548.45875	0.1137	R	−0.08 ± 0.08	−0.06 ± 0.07	0.10 ± 0.09	2455548.16822	0.7177	B	−0.12 ± 0.07	0.01 ± 0.04	0.12 ± 0.07
2455548.38332	0.9251	I	0.09 ± 0.09	−0.12 ± 0.10	0.15 ± 0.11	2455548.10586	0.6197	V	−0.16 ± 0.03	0.26 ± 0.03	0.30 ± 0.03
2455548.41294	0.9992	I	0.07 ± 0.12	0.18 ± 0.16	0.19 ± 0.16	2455548.12985	0.6574	V	−0.10 ± 0.03	0.26 ± 0.02	0.28 ± 0.02
2455548.43745	0.0605	I	0.01 ± 0.04	−0.14 ± 0.06	0.14 ± 0.06	2455548.15486	0.6967	V	−0.05 ± 0.08	0.20 ± 0.11	0.21 ± 0.11
2455549.17424	0.9025	B	0.10 ± 0.01	0.21 ± 0.01	0.23 ± 0.01	2455548.17301	0.7252	V	−0.22 ± 0.02	0.38 ± 0.01	0.44 ± 0.01
2455549.21096	0.9943	B	0.11 ± 0.01	−0.01 ± 0.01	0.11 ± 0.01	2455548.11270	0.6304	R	−0.48 ± 0.07	0.17 ± 0.08	0.51 ± 0.07
2455549.24345	0.0755	B	0.11 ± 0.04	−0.09 ± 0.03	0.14 ± 0.04	2455548.13635	0.6676	R	−0.08 ± 0.01	0.07 ± 0.01	0.10 ± 0.01
2455549.27437	0.1529	B	0.21 ± 0.04	0.40 ± 0.04	0.45 ± 0.04	2455548.15915	0.7034	R	−0.27 ± 0.03	0.36 ± 0.03	0.45 ± 0.02
2455549.18613	0.9322	V	0.13 ± 0.08	−0.02 ± 0.05	0.13 ± 0.08	2455548.17648	0.7306	R	−0.16 ± 0.02	0.25 ± 0.01	0.30 ± 0.01
2455549.21920	0.0149	V	0.27 ± 0.05	−0.01 ± 0.05	0.27 ± 0.05	2455548.11698	0.6372	I	−0.21 ± 0.11	−0.03 ± 0.08	0.21 ± 0.11
2455549.25207	0.0971	V	−0.08 ± 0.03	−0.36 ± 0.02	0.37 ± 0.02	2455548.14046	0.6741	I	−0.41 ± 0.13	0.22 ± 0.12	0.46 ± 0.13
2455549.28315	0.1748	V	−0.08 ± 0.07	0.13 ± 0.08	0.15 ± 0.09	2455548.16183	0.7076	I	0.20 ± 0.13	0.22 ± 0.13	0.30 ± 0.14
2455549.22681	0.0339	R	−0.07 ± 0.09	0.18 ± 0.12	0.19 ± 0.12	2455548.17916	0.7348	I	0.05 ± 0.01	0.27 ± 0.01	0.27 ± 0.01
2455549.25982	0.1165	R	0.14 ± 0.10	0.12 ± 0.09	0.19 ± 0.11						
2455549.20233	0.9727	I	−0.15 ± 0.13	−0.15 ± 0.12	0.21 ± 0.14						
2455549.23306	0.0496	I	0.01 ± 0.03	0.10 ± 0.04	0.10 ± 0.04						
2455549.26559	0.1309	I	0.11 ± 0.02	−0.20 ± 0.01	0.23 ± 0.01						
2455549.29799	0.2119	I	0.05 ± 0.01	0.10 ± 0.01	0.11 ± 0.01						

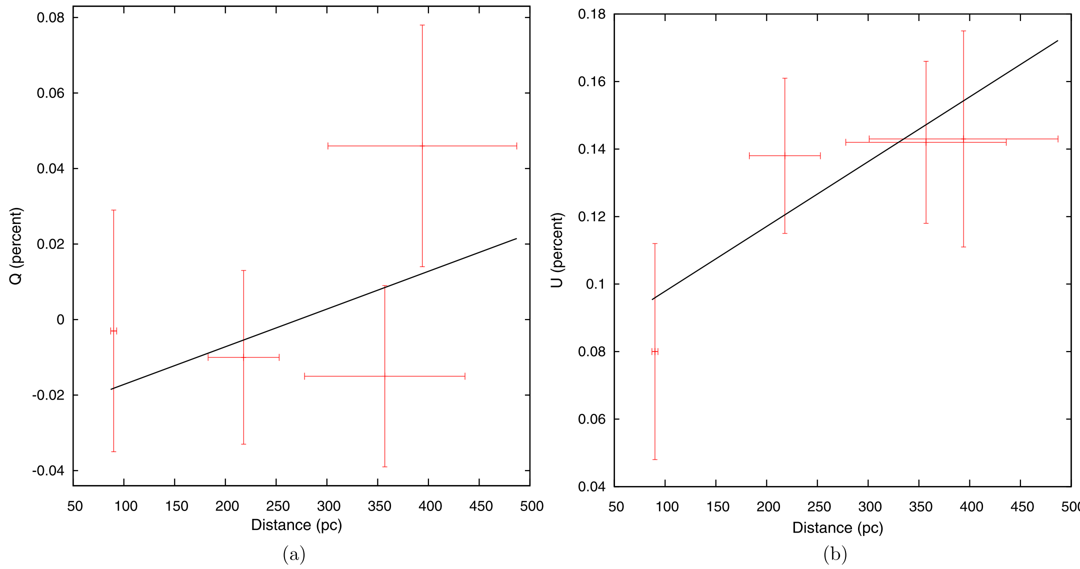

Fig. 9 (**a**) Q and (**b**) U versus distance plots using the stars distributed in a circular radius of 1.5° around FZ Ori (*continuous line* is best fit straight line to the data)

(2004) have also found similar results. Depth of secondary minima of the light curves of V407 Peg and LP UMa appear to be lower than the primary one. Further their secondary components temperatures are also found to be lesser than that of primary. The light curves of V407 Peg show a total eclipse configuration. However, the light curves of LP UMa have a partial eclipse nature. The present characteristics of the light cures of V407 Peg and LP UMa suggest that V407 Peg and LP UMa are A-type of W UMa contact binaries as has also been obtained respectively by Maciejewski et al. (2003) and Lee et al. (2014) and Csizmadia et al. (2003).

Our new times of light minimum of FZ Ori, V407 Peg and LP UMa used including other eclipse times compiled from the literature have resulted into the improvement of the period change analysis. The orbital periods of FZ Ori and LP UMa are found to increase with the rate of $2.28 \times 10^{-8}\ \mathrm{d\,yr^{-1}}$ and $1.25 \times 10^{-6}\ \mathrm{d\,yr^{-1}}$, respectively. The change in orbital period could be due to the mass transfer between the components of the system. The present analysis shows that mass has been transferred from primary to secondary in both the cases. In the W UMa type binaries the rates of change of orbital period are in the range from $\pm 10^{-9}$ to $\pm 10^{-6}\ \mathrm{d\,yr^{-1}}$ (Dryomova and Svechnikov 2006). The other few examples of W UMa binaries that show the increasing trend in their orbital period are FO Hya (Prasad et al. 2013), YY Eri (Kim et al. 1997), V839 Oph (Akalin and Derman 1997), AB And (Kalimeris et al. 1994), DK Cyg (Awadalla 1994), V401 Cyg (Herczeg 1993), V566 Oph (Maddox and Bookmyer 1981). The additional sinusoidal variation of FZ Ori may be interpreted as the light-time effect due to the existence of a tertiary companion. Under the assumption that the orbit of third companion is coplanar with the eclipsing pair, the mass of the tertiary companion was computed to be $0.56 M_\odot$. Using the empirical relations of Southworth (2009), the radius and effective temperature of the tertiary companion are calculated to be $R_3 = 0.58 R_\odot$ and $T_3 = 3726$ K, respectively. These correspond to a spectral type of about M1V and a bolometric luminosity of $0.058 L_\odot$. Further, the mass function, f(M_3) and a projected orbital semi-major axis, $a_{12} \sin i_3$ of the tertiary companion were found to be $0.014 M_\odot$ and 2.30 AU, respectively.

Our light curve modeling of FZ Ori shows the mass ratio of 0.86 ± 0.03, which is in between to that derived by Rukmini et al. (2001) and Byboth et al. (2004). However, the mass ratio for V407 Peg and LP UMa were adopted 0.256 ± 0.006 (Rucinski et al. 2008) and 0.886 ± 0.015 (Csizmadia et al. 2003), respectively. The high mass ratio systems FZ Ori and LP UMa have shallow contact configuration. However, their fill-out factors are of $\lesssim 15$ %, suggesting that the system is a marginal contact binary. Such contact binaries ($f \leqslant 10$ %) viz., V803 Aql (Samec et al. 1993), FG Sct (Bradstreet 1985), RW PsA (Lucy and Wilson 1979), XZ Leo (Niarchos et al. 1994), and S Ant (Russo et al. 1982) are indicators of evolution time scale into the contact stage (Liu et al. 2008). However, mass ratio and fill out factor of V407 Peg indicate that this is a contact binary system.

From the present light curve modeling, the temperature difference between the two components of FZ Ori, V407 Peg and LP UMa were found to be 43 K, 796 K and 873 K, respectively: the condition usually found in contact binaries. Lee et al. (2014), Deb and Singh (2011) and Maciejewski et al. (2003) have also found similar temperature difference

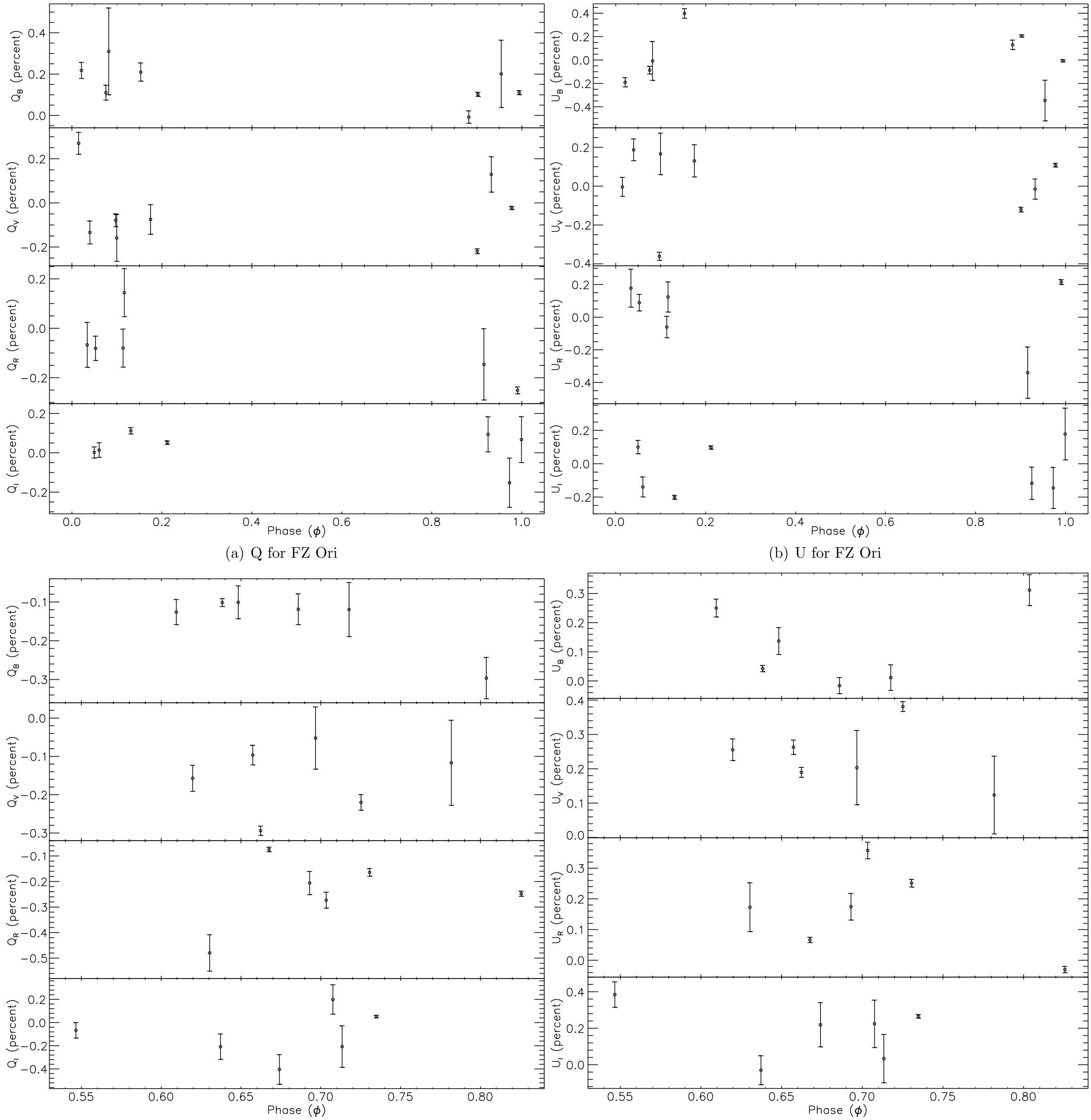

(a) Q for FZ Ori (b) U for FZ Ori

(c) Q for V407 Peg (d) U for V407 Peg

Fig. 10 Stokes parameters Q and U as functions of the orbital phase in the B, V, R and I bands running from top to bottom for ((**a**) and (**b**)) FZ Ori, and ((**c**) and (**d**)) V407 Peg

between the components and other features of light curve during the light curve modeling of V407 Peg system, excepting the orbital inclination presented in this paper differ much from those studies earlier than that of Lee et al. (2014). The existence of a tertiary component (see Table 4) in our study of V407 Peg is in agreement with the previous study made by Lee et al. (2014). While, for the LP UMa system, temperature difference between the components is slightly smaller than that determined by Csizmadia et al. (2003). To check the exact configuration, spectroscopically determined mass ratio is required as an input in the photometric light curve modeling but this was not available for the FZ Ori and LP UMa binary systems. Since the FZ Ori and LP UMa binary systems are showing partial eclipse nature and the absolute physical parameters are still uncertain yet, the solution is to be taken with caution. The precision radial-velocity curves will put our result on a strong footing. A precise spectroscopic radial velocity observations are needed for these binary systems.

We have inferred the mass, radius and luminosity of primary and secondary components of FZ Ori to be $M_1 = 1.167M_\odot$ and $M_2 = 1.0M_\odot$, $R_1 = 1.161R_\odot$ and $R_2 = 1.082R_\odot$, and $L_1 = 1.504L_\odot$ and $L_2 = 1.344L_\odot$, respectively. In case of V407 Peg and LP UMa, the determined parameters ($M_{1,2}$, $R_{1,2}$ and $L_{1,2}$) are found to be consistent with the earlier values reported in the literature. The computed distance modulus of FZ Ori yield the distance 237.68 pc for the system, in conformity with Zasche et al. (2009). While, the distance of V407 Peg is determined to be 327 ± 41 pc using the parallax of 3.06 ± 0.38 (Bilir et al. 2005). We have also found, similar to as obtained by Lee et al. (2014), the orbital inclination (in degree) of 90.32 ± 3.96 and a high degree of over-contact configuration of 84 % for V407 Peg system. Whereas, for the LP UMa system, the calculated distance modulus yield the distance to be 493.40 pc.

The first multi-band optical polarimetric observations of FZ Ori and V407 Peg show the average values in between 0.2–0.3 per cent. In W UMa-type binaries the degree of polarization was found up to 0.6 % (see Oshchepkov 1978; Piirola 1977). The variable polarization in W UMa type binaries have been found by Oshchepkov (1978), who suggested that the photospheric scattering, the reflection effect and scattering in a gaseous envelope or stream could be the possible sources of variable polarization. However, Pirola (1977) did not find any significant variability in the polarization and has suggested that the polarization due to gas streams may be a transient phenomenon. Furthermore, with help of polarimetric observations one can estimate the masses of the gas streams and mass loss rate of each component. Due to lack of data points with full phase coverage shape, we are unable to compute the masses of the gas streams, mass loss rate and rates of change of period. The polarimetric observations with good phase coverage are needed for such analysis and their comparison from photometric study. The well studied systems with large amplitude variations and developed gaseous envelopes; U Cep, U Sge, RW Tau, RY Per and β Lyr also show the variable polarization (Shakhovskoi 1965). These results demonstrate that data of this type form a new source of information on a number of physical and geometric properties of eclipsing binary systems.

Acknowledgements V. Prasad and D.C. Srivastava acknowledge the financial support received from UGC, Govt. of India under Rajeev Gandhi National Fellowship (No. F. 14-2(SC)/2010 (SA-III)). We are very grateful to Dr. Sukanta Deb, Delhi University and Dr. C. Eswaraiah, ARIES, Nainital for many helpful discussions. The authors would like to thank ARIES for making the telescope time available on the 104-cm Sampurnanand telescope for observations. V. Prasad also acknowledges to ARIES for providing hospitality, library and computational facilities. The authors thank the staff at ARIES for their active support during the course of observations. The use of the SIMBAD, ADS, 2MASS (which is a joint project of the University of Massachusetts and the Infrared Processing and Analysis Center/California Institute of Technology, funded by the National Aeronautics and Space Administration and the National Science Foundation) databases are gratefully acknowledged.

References

Akalin, A., Derman, E.: Astron. Astrophys. Suppl. Ser. **125**, 407 (1997)
Applegate, J.H.: Astrophys. J. **385**, 621 (1992)
Awadalla, N.S.: Astron. Astrophys. **289**, 137 (1994)
Binnendijk, L.: Vistas Astron. **12**, 217 (1970)
Bilir, S., Karataş, Y., Demircan, O., Eker, Z.: Mon. Not. R. Astron. Soc. **357**, 497 (2005)
Biro, I.B.: Inf. Bull. Var. Stars **4929** (2000)
Bonanos, A.Z.: Astrophys. J. **691**, 407 (2009)
Bradstreet, D.H.: Astrophys. J. Suppl. Ser. **58**, 413 (1985)
Byboth, K.N., Markworth, N.L., Bruton, W.B.: Inf. Bull. Var. Stars **5554** (2004)
Coughlin, J.L., Dale, H.A. III, Williamon, R.M.: Astron. J. **136**, 1089 (2008)
Cox, A.N.: Allen's astrophysical quantities (2000)
Csizmadia, Sz., Biro, I.B., Borkovits, T.: Astron. Astrophys. **403**, 637 (2003)
Cutri, R.M., Skrutskie, M.F., van Dyk, S., Beichman, C.A., Carpenter, J.M., Chester, T., Cambresy, L., Evans, T., Fowler, J., Gizis, J., Howard, E., Huchra, J., Jarrett, T., Kopan, E.L., Kirkpatrick, J.D., Light, R.M., Marsh, K.A., McCallon, H., Schneider, S., Stiening, R., Sykes, M., Weinberg, M., Wheaton, W.A., Wheelock, S., Zacarias, N.: 2MASS All Sky Catalog of point sources (2003)
Deb, S., Singh, H.P.: Mon. Not. R. Astron. Soc. **412**, 1787 (2011)
Dryomova, G.N., Svechnikov, M.A.: Astrophysics **49**, 358 (2006)
EI–Bassuny Alawy, A.A.: Astrophys. Space Sci. **207**, 171 (1993)
Eswaraiah, C., Pandey, A.K., Maheswar, G., Medhi Biman, J., Pandey, J.C., Ojha, D.K., Chen, W.P.: Mon. Not. R. Astron. Soc. **411**, 1418 (2011)
Figer, A.: Geos Cir. Eclips. Bin. **8** (1983)
Hoffmeister, C.: Astron. Nachr. **253**, 195 (1934)
Heiles, C.: Astron. J. **119**, 923 (2000)
Herczeg, T.J.: Publ. Astron. Soc. Pac. **105**, 911 (1993)
Irwin, J.B.: Astrophys. J. **116**, 211 (1952)
Irwin, J.B.: Astron. J. **64**, 149 (1959)
Kalimeris, A., Rovithis-Livaniou, H., Rovithis, P., Oprescu, G., Dumitrescu, A., Suran, M.D.: Astron. Astrophys. **291**, 765 (1994)
Kim, C.H., Jeong, J.H., Demircan, O., Muyesseroglu, J., Budding, E.: Astron. J. **114**, 2753 (1997)
Kwee, K.K., van Woerden, H.: Bull. Astron. Inst. Neth. **12**, 327 (1956)
Lanza, A.F., Rodonò, M.: Astron. Astrophys. **349**, 887 (1999)
Lanza, A.F., Rodonò, M.: Astron. Nachr. **323**, 424 (2002)
Le Brogne, J.F., Figer, A., Dumont, M.: Inf. Bull. Var. Stars **2566** (1984)
Lee, J.W., Park, J.H., Hong, K., Kim, S.L., Lee, C.U.: Astron. J. (2014). arXiv:1401.7489v1
Li, L., Zhang, F., Han, Z., Jiang, D., Jiang, T.: Mon. Not. R. Astron. Soc. **387**, 97 (2008)
Liu, L., Qian, S.-B., Zhu, L.-Y., He, J.-J., Yuan, J., Dai, Z., Liao, W., Zhang, J.: Publ. Astron. Soc. Jpn. **60**, 565 (2008)
Lucy, L.B., Wilson, R.E.: Astrophys. J. **231**, 502 (1979)
Lucy, L.B.: Z. Astrophys. **65**, 89 (1967)
Maciejewski, G., Karska, A., Niedzielski, A.: Inf. Bull. Var. Stars **5343**, 1 (2002)

Maciejewski, G., Ligeza, P., Karska, A.: Inf. Bull. Var. Stars **5400**, 1 (2003)
Maceroni, C., van't Veer, F.: Astron. Astrophys. **277**, 515 (1993)
Maceroni, C., Vilhu, O., van't Veer, F., van Hamme, W.: Astron. Astrophys. **288**, 529 (1994)
Maddox, W.C., Bookmyer, B.B.: Publ. Astron. Soc. Pac. **93**, 230 (1981)
Medhi, B.J., Maheswar, G., Brijesh, K., Pandey, J.C., Kumar, T.S., Sagar, R.: Mon. Not. R. Astron. Soc. **378**, 881 (2007)
Medhi, B.J., Maheswar, G., Pandey, J.C., Kumar, T.S., Sagar, R.: Mon. Not. R. Astron. Soc. **388**, 105 (2008)
Martin, B.E.: Inf. Bull. Var. Stars **4880** (2000)
Milone, E.E.: Astron. J. **73**, 708 (1968)
Niarchos, P.G., Hoffmann, M., Duerbeck, H.W.: Astron. Astrophys. **292**, 494 (1994)
O'Connell, D.J.K.: Publ. Riverv. Coll. Obs. **2**, 85 (1951)
Oshchepkov, V.A.: Ninfo **45**, 500 (1978)
Pandey, J.C., Medhi Biman, J., Sagar, R., Pandey, A.K.: Mon. Not. R. Astron. Soc. **396**, 1004 (2009)
Patel, M.K., Pandey, J.C., Savanov Igor, S., Prasad, V., Srivastava, D.C.: Mon. Not. R. Astron. Soc. **430**, 2154 (2013)
Prasad, V., Pandey, J.C., Patel, M.K., Srivastava, D.C.: New Astron. **20**, 52 (2013)
Paschke, A., Brat, L.: Open. Eur. J. Var. Stars **23**, 13 (2006)
Piirola, V.: Astron. Astrophys. **56**, 105 (1977)
Pojmanski, G.: Acta Astron. **47**, 467 (1997)
Pojmanski, G.: Acta Astron. **52**, 397 (2002)
Prša, A., Zwitter, T.: Astrophys. J. **628**, 426 (2005)
Qian, S., Ma, Y.: Publ. Astron. Soc. Pac. **113**, 754 (2001)
Rautela, B.S., Joshi, G.C., Pandey, J.C.: Bull. Astron. Soc. India **32**, 159 (2004)
Roberts, D.H., Lehar, J., Dreher, J.W.: Astron. J. **93**, 968 (1987)
Rovithis-Livaniou, H., Kranidiotis, A.N., Rovithis, P., Athanassiades, G.: Astron. Astrophys. **354**, 904 (2000)
Rucinski, S.M., Pribulla, T., Mochnacki, S.W., Liokumovich, E., Lu, W., DeBond, H., De Ridder, A., Karmo, T., Rock, M., Thomson, J.R., Ogłoza, W., Kaminski, K., Ligeza, P.: Astron. J. **136**, 586 (2008)
Rukmini, J., Vivekananda Rao, P., Ausekar, B.D.: Bull. Astron. Soc. India **29**, 323 (2001)
Rucinski, S.M., Duerbeck, H.W.: Publ. Astron. Soc. Pac. **109**, 1340 (1997)
Ruciński, S.M.: Acta Astron. **19**, 245 (1969)
Russo, G., Sollazzo, C., Maceroni, C., Milano, L.: Astron. Astrophys. Suppl. Ser. **47**, 211 (1982)
Samec, R.G., Su, W., Dewitt, J.R.: Publ. Astron. Soc. Pac. **105**, 1441 (1993)
Schlegel, D.J., Finkbeiner, D.P., Davis, M.: Astrophys. J. **500**, 525 (1998)
Schmidt, G.D., Elston, R., Lupie, O.L.: Astron. J. **104**, 1563 (1992)
Schaifers, K., Voigt, H.H.: J. Br. Astron. Assoc. **92**, 154 (1982)
Svechnikov, M.A., Kuznetsovs, Eh.F.: Catalog of approximate elements of eclipsing binaries, V/124 (1990)
Serkowski, K., Mathewson, D.S., Ford, V.L.: Astrophys. J. **196**, 261 (1975)
Shakhovskoi, N.M.: Sov. Astron. **8**, 833 (1965)
Shakhovskoy, N.M., Antonyuk, K.A.: Astrophysics **47**, 143 (2004)
Southworth, J.: Mon. Not. R. Astron. Soc. **394**, 272 (2009)
van Hamme, W.: Astron. J. **106**, 2096 (1993)
van Leeuwen, F.: Astron. Astrophys. **474**, 653 (2007)
Wang, J.M.: Astrophys. J. **434**, 277 (1994)
Webbink, R.F.: ASP Conf. Ser. **293**, 76 (2003)
Wilson, R.E., Devinney, E.J.: Astrophys. J. **166**, 605 (1971)
Wilson, R.E., Biermann, P.: Astron. Astrophys. **48**, 349 (1976)
Yang, Y., Liu, Q.: Publ. Astron. Soc. Pac. **115** 748 (2003)
Zasche, P.: Inf. Bull. Var. Stars **5991** (2011)
Zasche, P., Liakos, A., Niarchos, P., Wolf, M., Manimanis, V., Gazeas, K.: New Astron. **14**, 121 (2009)